

Constraining SMEFT BSM scenarios with EWPO and Δ_{CKM}

¹Mathew Thomas Arun ¹, ²Kuldeep Deka², ²Tripurari Srivastava³

¹*School of Physics, Indian Institute of Science Education and Research Thiruvananthapuram, Vithura, Kerala, 695551, India*

²*Department of Physics and Astrophysics, University of Delhi, Delhi 110007, India*

Abstract

Precision observables are well known for constraining most of the Beyond Standard Model (BSM) scenarios tightly. We present here a simple and comprehensive fitting framework for various BSM scenarios to these observables. We start with the fit of S , T and V parameter and their correlations using the Electroweak Precision Observables (EWPO) including the recent m_W measurement from CDF-II. Utilizing these observables, we also fit various New Physics (NP) scenarios consisting of different subsets of dimension-6 Standard Model Effective Field Theory (SMEFT) operators in the Warsaw basis out of a total of 10 appearing at tree level in EWPO. To further constrain these scenarios, we augment these observables with Δ_{CKM} measurement using 1-loop matching of the Low Energy Effective Field Theory (LEFT) to SMEFT operators at the Z-pole. We show that the inclusion of Δ_{CKM} constraint indeed results in stronger bounds on the SMEFT Wilson Coefficients. We also constrain the UV parameters of BSM extensions like Vectorlike leptons (VLL) and find out that such a minimal extension is in tension with the forward-backward asymmetry in b -sector (A_b^{FB}) and the recent measurement of M_W . In order to lift the two blind directions, which one encounters while fitting all the 10 SMEFT WCs at tree-level, we also include the LEP-II observables pertaining to the WW production and present the results for the fits with and without Δ_{CKM} constraint.

1 Introduction

The discovery of the Higgs at the LHC in 2012 [1] completes the Standard Model of particle physics (SM). On the other hand, the absence of any heavy resonances in the Run 2 of the Large Hadron Collider (LHC) implies that any physics beyond the Standard Model (BSM) is likely to be associated with an intrinsic energy scale significantly higher than the electroweak scale. Interestingly, however, a few discrepancies have been seen in low energy experiments like the $(g - 2)$ of the muon [2–6], flavor anomalies [7–10], the Cabibbo anomaly [11] and the recent CDF anomaly in W boson mass [12]. Given the elusiveness of New Physics at collider experiments, there is a huge motivation to understand the nature of various anomalies in a model-independent Effective Field Theory formalism. In our study, a class of New Physics effects are included by extending SM with higher dimensional operators which are invariant under the SM gauge group. While the full set of such operators – together constituting the Standard Model Effective Field Theory (SMEFT) [13–18] – is large, we concentrate on a subset that are likely to play leading roles in addressing the Cabibbo and CDF anomalies as well as the Electroweak Precision Observables (EWPO). Being well measured at LEP [19–23] along with SLAC and Tevatron [24], the precise measurements of Electroweak Precision Observables (EWPO) strongly constrain the scales of these SMEFT operators.

¹thomas.mathewarun@gmail.com

²kuldeepdeka.physics@gmail.com

³tripurarisri022@gmail.com

In the last decade, studies on SMEFT have gained significant amount of attention. Many studies have been performed to analyze the SMEFT in the context of EWPO [25–34]. At tree level in the Warsaw basis [15], eight SMEFT WCs out of a total of ten contributing to the EWPO can be constrained [35]. It has also been found that the inclusion of WW production data at LEP-II, allows for constraining all the ten WCs [35, 35, 36]. Moreover, there have also been numerous studies on the global fit of EWPO in the context of SMEFT [30, 34, 36, 37].

The recent measurement of W boson mass [12], $M_W = 80,433.5 \pm 9.4$ MeV, disagrees with the SM prediction, $M_W = 80,360 \pm 6$ MeV, at 7σ level. The new combined world average, calculated from the uncorrelated average of all m_W measurements at Tevatron, LEP-II and the LHC, now lies at $M_W = 80,413.3 \pm 9$ MeV [38]. Several studies have been conducted to address the impact of this new measurement on the Global EW fit in terms of the oblique parameters [39–42] and also assuming the SMEFT framework [38, 43, 44, 44–49]. Models such as Technicolor models, Extradimensions, Composite Higgs or Little Higgs scenarios, SU(2) Triplet Scalar Extensions [50], Models with VLQ [51], Two Higgs Doublet Models [39] among many others [40, 52–55] have also been proposed to address this.

Apart from this, anomalies have been reported in low-energy measurements. These are studied using Low-energy Effective Field Theory (LEFT) description of the Standard Model. In particular, in this study, we have considered the beta decay and other semileptonic processes that contribute to the deviation in first row unitarity of the CKM matrix ($|V_{ud}|^2 + |V_{us}|^2 - 1$, neglecting the tiny $|V_{ub}|^2$ contributions) in the LEFT basis. Also known as Δ_{CKM} or Cabibbo anomaly, this quantity shows a discrepancy of 2σ . Since Δ_{CKM} and electro-weak precision tests crucially depend on the measured value of G_F , albeit at different scales, these measurements are connected and have to be taken together while constraining any New Physics. To that end, we match these LEFT operators with SMEFT at 1-loop at the Z boson scale and obtain experimental constraints on the Wilson Coefficients (WCs) of the dimension-6 SMEFT operators.

In this article, we perform an all-parameter fit which takes into account all the 10 WCs affecting the EWPO at tree-level, with the recent CDF-II M_W mass measurement and Δ_{CKM} constraint. Along with these two observables, A_b^{FB} and A_l^{SLD} too play significant roles in these fits, since both have a long-standing discrepancy of more than 2σ with respect to the SM predictions. However, we encounter two blind directions as the EWPO can only constrain 8 independent combinations of the WCs. Addition of Δ_{CKM} also does not help in lifting the blind directions. Rather, this forces us to use LEP-II data, where the presence of W-W production channel breaks the two blind directions, enabling us to constrain all the 10 WCs of our interest. In order to realise these fits, we have written our own code from the scratch in *Mathematica*, making it highly expandable and modular in design. To make it more versatile and user-friendly, we are also working on its easy integration with other publicly available packages for various SMEFT and New Physics calculations like CoDEx [56], SmeftFR [57], SMEFTsim [58], DsixTools [59], Rosetta [60], FeynMG [61], FeynRules [62], FeynCalc [63], FeynArts [64] *etc.*, other LEFT-SMEFT matching tools [65] and tools for computing Electroweak chiral amplitudes (Higgs EFT) [66].

In the SMEFT parametrisation, we also consider certain subsets of operators affecting the observables of our interest and perform the fit to constrain their WCs. Depending on the UV complete scenarios, typically only a subset of all the WCs contributes significantly to a set of well measured low energy observables. One such fit looks at the scenario where the operators common to the M_W and Δ_{CKM} are the ones carrying the imprint of the New Physics. Another New Physics scenario considered here is the set of WCs which appear in the expression for M_W at the tree-level.

We also perform a fit for the vector-like lepton models which are popular for their ability to address the discrepancy in muon $(g-2)$ and providing masses to the SM neutrinos through the seesaw mechanism. By matching these models to SMEFT at the tree-level, we perform the fit where the WCs now carry the imprints of couplings and the mass-scale of these new leptons. It also enables us to constrain the UV parameters of the model.

Moreover, we have used S , T and V [67–69] to parametrise the New Physics contribution to EWPO. With the assumption that there are no additional electroweak gauge bosons and that new physics coupling to light fermions are suppressed, S and T (along with U , contributions to which from majority of new physics scenarios are small and generated at SMEFT in dimension-8) parametrise the new physics effects in the vacuum polarisation diagrams of the electroweak gauge bosons. If the presence of New Physics also leads to changing of the weak coupling constant G_F , it can be parametrised by the inclusion of V parameter along with S and T [70]. Since the Cabibbo anomaly can only be explained by adjusting the V parameter, this analysis is rendered all the more important.

This paper is organized as follows: In the next section, we revisit the contributions of dimension-6 operators to the shift in fermion couplings to gauge-bosons at leading order. In section [3], we briefly discuss the near Z pole precision observables (EWPO) and the observables arising due to WW production (LEP-II). We then discuss the contributions of the SMEFT operators to muon and beta decay as obtained by matching with LEFT at one loop (in section) [4] and discuss the fitting framework in section [5]. Further, we analyze various model independent frameworks, using S , T , V and the subsets of dimension-6 operators affecting the EWPO and Δ_{CKM} . Finally, in section [6] we summarize the results.

2 SMEFT contributions to Electroweak Fit

The low-energy effects of massive BSM particles can be approximated by integrating out the corresponding fields to obtain higher-dimensional interactions between the SM fields. In such an approach, the SM can be regarded as an effective theory whose known renormalizable interactions are supplemented by higher-order terms scaled by inverse powers of the BSM mass scale. The consequent effective Lagrangian can, then, be written in the form

$$\mathcal{L}_{eff} = \mathcal{L}_{SM} + \sum_{d=5}^{\infty} \sum_{i=1}^n \frac{\mathcal{C}_i^d}{\Lambda^{d-4}} O_i^d, \quad (1)$$

where d represents the dimension of the operator and i runs over all the relevant set of operators at a particular dimension. The operators O_i^d are all $SU(3) \times SU(2)_L \times U(1)_Y$ invariant with all of the effects of the BSM physics residing in the WCs \mathcal{C}_i^d . In our work, we assume the WCs to be real to eliminate any new sources of CP violation and use the Warsaw basis [15] to parametrise them.

The EWPO of our primary interest are the Z and W pole observables and there are 10 six dimensional operators which contribute to these observables at the tree level. We collect these operators in Table 1, where H is the $SU(2)_L$ Higgs doublet, τ^a are the Pauli matrices, $D_\mu = \partial_\mu + ig_s T^A G_\mu^A + ig_2 \frac{\tau^a}{2} W_\mu^a + ig_1 Y B_\mu$, q is the $SU(2)_L$ quark-doublet with $q^T = (u_L, d_L)$, l is the $SU(2)_L$ lepton-doublet with $l^T = (\nu_L, e_L)$, $W_{\mu\nu}^a$ is the $SU(2)_L$ field strength with $W_{\mu\nu}^a = \partial_\mu W_\nu^a - \partial_\nu W_\mu^a - g_2 \epsilon^{abc} W_\mu^b W_\nu^c$ and $B_{\mu\nu}$ is the $U(1)_Y$ field strength with $B_{\mu\nu} = \partial_\mu B_\nu - \partial_\nu B_\mu$. The other definitions include: $H^\dagger i \overleftrightarrow{D}_\mu H = iH^\dagger(D_\mu H) - i(D_\mu H)^\dagger H$, and $H^\dagger i \overleftrightarrow{D}_\mu^a H = iH^\dagger \tau^a D_\mu H - i(D_\mu H)^\dagger \tau^a H$.

\mathcal{O}_{HD}	$(H^\dagger D^\mu H)^* (H^\dagger D_\mu H)$	\mathcal{O}_{HWB}	$(H^\dagger \tau^a H) W_{\mu\nu}^a B^{\mu\nu}$
\mathcal{O}_{ll}	$(\bar{l}\gamma_\mu l)(\bar{l}\gamma^\mu l)$	\mathcal{O}_{He}	$(H^\dagger i\overleftrightarrow{D}_\mu H)(\bar{e}\gamma^\mu e)$
\mathcal{O}_{Hu}	$(H^\dagger i\overleftrightarrow{D}_\mu H)(\bar{u}\gamma^\mu u)$	\mathcal{O}_{Hd}	$(H^\dagger i\overleftrightarrow{D}_\mu H)(\bar{d}\gamma^\mu d)$
\mathcal{O}_{Hq_3}	$(H^\dagger i\overleftrightarrow{D}_\mu^a H)(\bar{q}\tau^a\gamma^\mu q)$	\mathcal{O}_{Hq_1}	$(H^\dagger i\overleftrightarrow{D}_\mu H)(\bar{q}\gamma^\mu q)$
\mathcal{O}_{Hl_3}	$(H^\dagger i\overleftrightarrow{D}_\mu^a H)(\bar{l}\tau^a\gamma^\mu l)$	\mathcal{O}_{Hl_1}	$(H^\dagger i\overleftrightarrow{D}_\mu H)(\bar{l}\gamma^\mu l)$

Table 1: Dimension-6 operators in Warsaw basis contributing to the EWPO at tree level.

In order to get the theoretical predictions from the Electroweak precision Data pertaining to the pole observables, we first fix our choice of input parameters⁴, namely, the fine structure constant $\hat{\alpha}_e$ from the low energy limit of electron Compton scattering, the Fermi constant in muon decays \hat{G}_F and the measured Z mass (\hat{m}_Z). At the tree level, one can then define the effective (measurable) mixing angle

$$s_W^2 = \frac{1}{2} - \frac{1}{2} \sqrt{1 - \frac{4\pi\hat{\alpha}_e}{\sqrt{2}\hat{G}_F\hat{m}_Z^2}}. \quad (2)$$

The value of the $SU(2)_L$ gauge coupling can be taken as:

$$\hat{g}_2 s_W = 2\sqrt{\pi}\hat{\alpha}_e^{1/2}. \quad (3)$$

The effective measured vacuum expectation value (vev) in the SM can be defined as $\hat{v}^2 = 1/\sqrt{2}\hat{G}_F$.

Once we allow for these new SMEFT operators, the gauge sector gets modified. To have canonical kinetic term, we must then effect a redefinition of fields and couplings. The redefined quantities are [71]:

$$\begin{aligned} \overline{W}_\mu^a &\equiv (1 - \mathcal{C}_{HW}v^2/\Lambda^2)W_\mu^a \\ \overline{B}_\mu &\equiv (1 - \mathcal{C}_{HB}v^2/\Lambda^2)B_\mu \\ \overline{g}_2 &\equiv (1 + \mathcal{C}_{HW}v^2/\Lambda^2)g_2 \\ \overline{g}_1 &\equiv (1 + \mathcal{C}_{HB}v^2/\Lambda^2)g_1, \end{aligned} \quad (4)$$

such that $\overline{W}_\mu\overline{g}_2 \approx W_\mu g_2$ and $\overline{B}_\mu\overline{g}_1 \approx B_\mu g_1$. The masses of the W and Z fields to $\mathcal{O}(\Lambda^{-2})$ are [71],

$$\begin{aligned} M_W^2 &= \frac{\overline{g}_2^2 v^2}{4}, \\ M_Z^2 &= \frac{(\overline{g}_1^2 + \overline{g}_2^2)v^2}{4} + \frac{v^4}{\Lambda^2} \left(\frac{1}{8}(\overline{g}_1^2 + \overline{g}_2^2)\mathcal{C}_{HD} + \frac{1}{2}\overline{g}_1\overline{g}_2\mathcal{C}_{HWB} \right). \end{aligned} \quad (5)$$

The induced change to the effective 4-fermion operator governing the decay of the muon alters the relation between the vev, v , and the Fermi constant \hat{G}_F to

$$\hat{G}_F \equiv \frac{1}{\sqrt{2}v^2} - \frac{1}{\sqrt{2}\Lambda^2}\mathcal{C}_{ll} + \frac{\sqrt{2}}{\Lambda^2}\mathcal{C}_{Hl_3}. \quad (6)$$

Using dimensionful WCs $C_i = \mathcal{C}_i/\Lambda^2$ (in TeV^{-2}) for the subsequent parts, the shift in M_Z^2 can then be written as:

$$\delta M_Z^2 \equiv \frac{1}{2\sqrt{2}} \frac{\hat{m}_Z^2}{\hat{G}_F} C_{HD} + \frac{2^{1/4}\sqrt{\pi}\sqrt{\hat{\alpha}_e}\hat{m}_Z}{\hat{G}_F^{3/2}} C_{HWB}. \quad (7)$$

⁴The choice of this particular combination is inspired from the higher experimental precision in their determination as compared to the other parameters in the SM

where \hat{m}_Z is the input parameter. The kinetic mixing introduced by the operator \mathcal{O}_{HWB} leads to a shift in the usual ($s_W \equiv \sin \theta_W$) mixing angle of the SM given by

$$\delta s_W^2 = -v^2 \frac{s_W c_W}{c_W^2 - s_W^2} \left[2s_W c_W \left(\delta v + \frac{1}{4} C_{HD} \right) + C_{HWP} \right]. \quad (8)$$

We relate the Lagrangian parameters \bar{g}_2, \bar{g}_1 to the input parameters at tree level via

$$\bar{g}_1^2 + \bar{g}_2^2 = 4 \sqrt{2} \hat{G}_F \hat{m}_Z^2 \left(1 - \sqrt{2} \delta G_F - \frac{\delta M_Z^2}{\hat{m}_Z^2} \right), \quad (9)$$

$$\bar{g}_2^2 = \frac{4 \pi \alpha_e}{s_W^2} \left[1 + \frac{\delta s_W^2}{s_W^2} + \frac{c_W}{s_W} \frac{1}{\sqrt{2} \hat{G}_F} C_{HWP} \right]. \quad (10)$$

Expressing \bar{M}_W^2 in terms of the inputs parameters we get

$$\bar{M}_W^2 = \hat{m}_W^2 \left(1 + \frac{\delta s_W^2}{s_W^2} + \frac{c_W}{s_W \sqrt{2} \hat{G}_F} C_{HWP} + \sqrt{2} \delta G_F \right) = \hat{m}_W^2 - \delta M_W^2, \quad (11)$$

where $\delta M_W^2 = -\hat{m}_W^2 \left(\frac{\delta s_W^2}{s_W^2} + \frac{c_W}{s_W \sqrt{2} \hat{G}_F} C_{HWP} + \sqrt{2} \delta G_F \right)$ and $\hat{m}_W^2 = c_W^2 \hat{m}_Z^2$.

The effective axial and vector couplings of the Z boson are now defined as

$$\mathcal{L}_{Z,eff} = g_{Z,eff} \left(J_\mu^{Z\ell} Z^\mu + J_\mu^{Z\nu} Z^\mu + J_\mu^{Zu} Z^\mu + J_\mu^{Zd} Z^\mu \right), \quad (12)$$

where $g_{Z,eff} = -2^{5/4} \sqrt{\hat{G}_F} \hat{m}_Z$, and $(J_\mu^{Zx})^{ij} = \bar{\psi}_i \gamma_\mu \left[(\bar{g}_V^x)_{eff}^{ij} - (\bar{g}_A^x)_{eff}^{ij} \gamma_5 \right] \psi_j$ for $\psi = \{u, d, \ell, \nu\}$. In general, these currents are matrices in flavour space. When we restrict our attention to the case of a minimal flavour violating (MFV) scenario, $(J_\mu^{Zx})_{ij} \simeq (J_\mu^{Zx}) \delta_{ij}$. The effective axial and vector couplings are modified from the SM values by a shift defined as

$$\delta(g_{V,A}^x)_{ij} = (\bar{g}_{V,A}^x)_{ij}^{eff} - (g_{V,A}^x)_{ij}^{SM}, \quad (13)$$

The tree level couplings are usual SM relations,

$$g_R^{Zf} = -s_W^2 Q_f \quad \text{and} \quad g_L^{Zf} = T_3^f - s_W^2 Q_f \quad (14)$$

with $T_3^f = \pm \frac{1}{2}$. The full SMEFT contributions to the effective couplings are shown in Table 2.

For the charged currents, we define

$$\mathcal{L}_{W,eff} = -\frac{\sqrt{2} \pi \alpha_e}{s_W} \left[(J_\mu^{W\pm,\ell})_{ij} W_\pm^\mu + (J_\mu^{W\pm,q})_{ij} W_\pm^\mu \right], \quad (15)$$

where in the SM one has

$$(J_\mu^{W+,\ell})_{ij} = \bar{\nu}_i \gamma^\mu \left(\bar{g}_V^{W+,\ell} - \bar{g}_A^{W+,\ell} \gamma_5 \right) \ell_j, \quad (16)$$

$$(J_\mu^{W-,\ell})_{ij} = \bar{\ell}_i \gamma^\mu \left(\bar{g}_V^{W-,\ell} - \bar{g}_A^{W-,\ell} \gamma_5 \right) \nu_j. \quad (17)$$

The contribution of these shifts to the observables of our interest can then be calculated [25, 28, 28, 29, 31, 72, 73].

$\delta(g_V^\ell)$	$\delta\bar{g}_Z(g_V^\ell)^{SM} - \frac{1}{4\sqrt{2}\hat{G}_F}(C_{He} + C_{Hl_1} + C_{Hl_3}) - \delta s_W^2,$
$\delta(g_A^\ell)$	$\delta\bar{g}_Z(g_A^\ell)^{SM} + \frac{1}{4\sqrt{2}\hat{G}_F}(C_{He} - C_{Hl_1} - C_{Hl_3}),$
$\delta(g_V^\nu)$	$\delta\bar{g}_Z(g_V^\nu)^{SM} - \frac{1}{4\sqrt{2}\hat{G}_F}(C_{Hl_1} - C_{Hl_3})$
$\delta(g_A^\nu)$	$\delta\bar{g}_Z(g_A^\nu)^{SM} - \frac{1}{4\sqrt{2}\hat{G}_F}(C_{Hl_1} - C_{Hl_3})$
$\delta(g_V^u)$	$\delta\bar{g}_Z(g_V^u)^{SM} + \frac{1}{4\sqrt{2}\hat{G}_F}(-C_{Hq_1} + C_{Hq_3} - C_{Hu}) + \frac{2}{3}\delta s_W^2$
$\delta(g_A^u)$	$\delta\bar{g}_Z(g_A^u)^{SM} - \frac{1}{4\sqrt{2}\hat{G}_F}(C_{Hq_1} - C_{Hq_3} - C_{Hu})$
$\delta(g_V^d)$	$\delta\bar{g}_Z(g_V^d)^{SM} - \frac{1}{4\sqrt{2}\hat{G}_F}(C_{Hq_1} + C_{Hq_3} + C_{Hd}) - \frac{1}{3}\delta s_W^2$
$\delta(g_A^d)$	$\delta\bar{g}_Z(g_A^d)^{SM} + \frac{1}{4\sqrt{2}\hat{G}_F}(-C_{Hq_1} - C_{Hq_3} + C_{Hd})$
$\delta(g_V^{W^\pm, \ell}) = \delta(g_A^{W^\pm, \ell})$	$\frac{1}{2\sqrt{2}\hat{G}_F}\left(C_{Hl_3} + \frac{1}{2}\frac{c_W}{s_W}C_{HWB}\right) + \frac{1}{4}\frac{\delta s_W^2}{s_W^2}$
$\delta(g_V^{W^\pm, q}) = \delta(g_A^{W^\pm, q})$	$\frac{1}{2\sqrt{2}\hat{G}_F}\left(C_{Hq_3} + \frac{1}{2}\frac{c_W}{s_W}C_{HWB}\right) + \frac{1}{4}\frac{\delta s_W^2}{s_W^2}$

Table 2: Anomalous fermion couplings at LO

3 W and Z pole observables of interest

In this section, we briefly discuss the contributions from SMEFT to the observables considered. Our list of EWPO includes [19, 31, 38, 74]:

$$M_W, \Gamma_W, \Gamma_Z, \sigma_h, R_l, A_l^{FB}, R_b, R_c, A_b^{FB}, A_c^{FB}, A_b, A_c, A_l, A_l^{SLD}, BR_{W \rightarrow \nu l}. \quad (18)$$

In the SMEFT, at tree level, the decay width of Z boson to fermions can be given by:

$$\bar{\Gamma}(Z \rightarrow f\bar{f}) = \frac{\sqrt{2}\hat{G}_F\hat{m}_Z^3 N_c}{3\pi} \left(|\bar{g}_V^f|^2 + |\bar{g}_A^f|^2 \right), \quad (19)$$

$$\bar{\Gamma}(Z \rightarrow \text{Had}) = 2\bar{\Gamma}(Z \rightarrow u\bar{u}) + 3\bar{\Gamma}(Z \rightarrow d\bar{d}), \quad (20)$$

with our chosen normalization of $\bar{g}_V^f = T_3/2 - Q^f \bar{s}_\theta^2$ and $\bar{g}_A^f = T_3/2$ where $T_3 = 1/2$ for u_i, ν_i and $T_3 = -1/2$ for d_i, ℓ_i and $Q^f = \{-1, 2/3, -1/3\}$ for $f = \{\ell, u, d\}$. Here, N_C is 3 for quarks and 1 for leptons. The modification of the decay widths in the SMEFT compared to the situation in the SM introduces corrections of the form [25, 27–29, 72]

$$\delta\Gamma_{Z \rightarrow \ell\bar{\ell}} = \frac{\sqrt{2}\hat{G}_F\hat{m}_Z^3}{6\pi} \left[-\delta g_A^\ell + (-1 + 4s_W^2) \delta g_V^\ell \right], \quad (21)$$

$$\delta\Gamma_{Z \rightarrow \nu\bar{\nu}} = \frac{\sqrt{2}\hat{G}_F\hat{m}_Z^3}{6\pi} [\delta g_A^\nu + \delta g_V^\nu], \quad (22)$$

$$\delta\Gamma_{Z \rightarrow \text{Had}} = 2\delta\Gamma_{Z \rightarrow u\bar{u}} + 3\delta\Gamma_{Z \rightarrow d\bar{d}}, \quad (23)$$

$$= \frac{\sqrt{2}\hat{G}_F\hat{m}_Z^3}{\pi} \left[\delta g_A^u - \frac{1}{3}(-3 + 8s_W^2) \delta g_V^u - \frac{3}{2}\delta g_A^d + \frac{1}{2}(-3 + 4s_W^2) \delta g_V^d \right], \quad (24)$$

$$\delta\Gamma_Z = 3\delta\Gamma_{Z\rightarrow\ell\bar{\ell}} + 3\delta\Gamma_{Z\rightarrow\nu\bar{\nu}} + \delta\Gamma_{had}, \quad (25)$$

$$= \frac{\sqrt{2}\hat{G}_F\hat{m}_Z^3}{2\pi} \left[\delta g_A^\nu + \delta g_V^\nu - \delta g_A^\ell + (-1 + 4s_W^2) \delta g_V^\ell, \right. \\ \left. + 2\delta g_A^u - \frac{2}{3}(-3 + 8s_W^2) \delta g_V^u - 3\delta g_A^d + (-3 + 4s_W^2) \delta g_V^d \right], \quad (26)$$

Here: $\bar{\Gamma}(Z \rightarrow f\bar{f}) = \Gamma_{Z\rightarrow f\bar{f}}^{SM} + \delta\Gamma_{Z\rightarrow f\bar{f}}$ for all f and the same kind of relation holds for $\bar{\Gamma}_{Z\rightarrow Had}$.

In terms of the partial widths in the SM at the Z pole, $\sigma_{e^+e^-\rightarrow had}$ has the expression

$$\bar{\sigma}_h^0 = 12\pi \frac{\bar{\Gamma}_{Z\rightarrow e\bar{e}}\bar{\Gamma}_{Z\rightarrow Had}}{|\bar{\omega}(M_Z^2)|^2}, \quad (27)$$

with $\bar{\Gamma}_{Z\rightarrow e\bar{e}}$, $\bar{\Gamma}_{Z\rightarrow Had}$ being the decay widths in SM. In the narrow-width approximation, $\bar{\omega}(M_Z^2) = \bar{M}_Z \bar{\Gamma}_Z$. The expression for its shift is relegated to Appendix 7.

The shift of the ratios of decay rates defined in the SM as $R_f^0 = \frac{\Gamma_{had}}{\Gamma_{Z\rightarrow f\bar{f}}}$ (where f can be a charged lepton ℓ or a neutrino) follows from

$$\delta R_f^0 = \frac{1}{(\Gamma(Z \rightarrow f\bar{f})^2)_{SM}} \left[\delta\Gamma_{Z\rightarrow Had}(\Gamma(Z \rightarrow f\bar{f}))_{SM} - \delta\Gamma_{Z\rightarrow f\bar{f}}(\Gamma(Z \rightarrow Had)_{SM}) \right], \quad (28)$$

and we can then write $\bar{R}_f^0 = R_f^0 + \delta R_f^0$. For an identified quark, the inverse ratio is used. The forward backward asymmetry for a $2 \rightarrow 2$ scattering process is defined as

$$A_{FB} = \frac{\sigma_F - \sigma_B}{\sigma_F + \sigma_B}. \quad (29)$$

If θ is the angle between incoming lepton ℓ and outgoing fermion f then, σ_F is the cross-section defined in the region $\theta \in [0, \pi/2]$ and σ_B is the cross-section defined in the region $\theta \in [\pi/2, \pi]$. In terms of the couplings, it can also be expressed as $A_{FB}^{0,f} = \frac{3}{4}A_e A_f$ where

$$A_e = 2 \frac{g_V^\ell g_A^\ell}{(g_V^\ell)^2 + (g_A^\ell)^2}, \quad A_f = 2 \frac{g_V^f g_A^f}{(g_V^f)^2 + (g_A^f)^2}. \quad (30)$$

Once we include the SMEFT operators, the Z couplings receive corrections (given in Table 2) which in turn, induces corrections to these observables. The expressions for the corrections pertaining to some of the observables have also been shown in Appendix 7 in detail.

The partial W width within the SMEFT is given by [29, 36]:

$$\bar{\Gamma}_{W\rightarrow\bar{f}_i f_j} = \Gamma_{W\rightarrow\bar{f}_i f_j}^{SM} + \delta\Gamma_{W\rightarrow\bar{f}_i f_j}, \quad (31)$$

$$\Gamma_{W\rightarrow\bar{f}_i f_j}^{SM} = \frac{N_C |V_{ij}^f|^2 \sqrt{2}\hat{G}_F \hat{m}_W^3}{12\pi}, \quad (32)$$

$$\delta\Gamma_{W\rightarrow\bar{f}_i f_j} = \frac{N_C |V_{ij}^f|^2 \sqrt{2}\hat{G}_F \hat{m}_W^3}{12\pi} \left(4\delta g_{V/A}^{W\pm,f} + \frac{1}{2} \frac{\delta m_W^2}{\hat{m}_W^2} \right). \quad (33)$$

V_{ij}^f are CKM or PMNS mixing matrix elements as the case may be. Summing over all the modes we can compute the contribution to the total decay width.

3.1 LEP-II data

One issue with using just the data from EWPO is that they can only constrain 8 linear combination of the WCs out of a total of 10 WCs which affect the EWPO at tree-level, resulting in two blind directions. The origin of this can be traced to the fact that there is a reparametrisation invariance where the fields and the couplings have the property: $\mathcal{F}, g \rightarrow \mathcal{F}'(1+\epsilon)g'(1-\epsilon)$ [35,36,75] for the $2 \rightarrow 2$ scattering processes. In order to break this invariance, one has to go to $2 \rightarrow 4$ scattering processes. These were suppressed at LEP-I (off-shell processes) but realised in LEP-II due to the possibility of having resonant production of W^+ and W^- . Pair produced W 's can then further decay leptonically to (ℓ, ν_ℓ) or hadronically to (j, j) . In addition to breaking the invariance, measurement of these four fermions final states also provide additional observables for electroweak precision studies. The contributions from the SMEFT to these processes have been calculated for assuming both resonant and non-resonant processes. Details of these observables and their χ^2 analysis have also been studied in Ref. [30].

4 Going Beyond EWPO: Δ_{CKM}

The aim of this section is to understand the SMEFT operators that enter the LEFT observables like muon decay and β -decay which are relevant in electroweak precision study. In [76], the authors studied the maximal deviation of Δ_{CKM} allowed by electroweak precision measurements. Their study was specific to the combination of $\mathcal{O}_l, \mathcal{O}_{lq_3}, \mathcal{O}_{Hl_3}$ and \mathcal{O}_{Hq_3} SMEFT operators that contribute at tree-level to the Δ_{CKM} constraint, in the limit of $U(3)^5$ invariance.

Since the SMEFT operators \mathcal{O}_{HD} and \mathcal{O}_{HWB} , among others, given in Table 1, are crucial to electroweak study, here we ask the question regarding how much they influence Δ_{CKM} at 1-loop order. Moreover, the LHC direct bounds on these operators are not severe as those on the leptonic ones. In such a scenario, it becomes important to understand these operators and their contributions in low-energy observables. Hence, in this section, we match the muon decay and β -decay to 1-loop order [65,77,78], thus including the SMEFT operators given in Table 1 in the Δ_{CKM} constraint. In particular, the operator $[\mathcal{O}_{lq_3} \equiv (\bar{l}\tau^a\gamma_\mu l)(\bar{q}\tau^a\gamma^\mu q)]$ appearing at tree-level in Δ_{CKM} is neglected as it doesn't impact the EWPO if we neglect the off-shell processes.

Assuming a $U(3)^5$ flavour symmetry [76], the correction to CKM unitarity is given by

$$\Delta_{CKM} = |V_{ud}|^2 + |V_{us}|^2 + |V_{ub}|^2 - 1 . \quad (34)$$

Here, V_{ub} is very small and can be neglected. The CKM matrix element $|V_{ud}|$ is precisely measured from the study of super allowed $0^+ \rightarrow 0^+$ beta decay. A crucial input for the correct determination is the precision of G_F . To understand the New Physics contribution to G_F , let us begin by studying the muon decay process.

4.1 Muon Decay

At low energies, the Lagrangian density that leads to the process $\mu \rightarrow e\bar{\nu}_e\nu_\mu$ is given by

$$\mathcal{L}_\mu = L_{\nu e}^{V,LL}(\bar{\nu}_{L\mu}\gamma^\mu\nu_{Le})(\bar{e}_L\gamma_\mu\mu_L) + L_{\nu e}^{V,LR}(\bar{\nu}_{L\mu}\gamma^\mu\nu_{Le})(\bar{e}_R\gamma_\mu\mu_R) , \quad (35)$$

where, all the WCs are measured at the muon mass scale.

At tree-level, the matching of the LEFT Lagrangian with the SMEFT one gives,

$$L_{\nu e \text{ tree}}^{V,LL} = -\frac{2}{v^2} + \left(C_{ll(1,2,2,1)} + C_{ll(2,1,1,2)} - 2(C_{Hl_3(2,2)} + C_{Hl_3(1,1)}) \right) U_{(1,1)} U_{(2,2)}^\dagger, \quad (36)$$

where U is the PMNS matrix. At 1-loop level, the matching of LEFT Lagrangian with the SMEFT Lagrangian gives,

$$\begin{aligned} L_{\nu e \text{ 1-loop}}^{V,LL} = & -1.48946 \log \mu_W^2 - 6.8206 \log \mu_W^2 \left(0.024(C_{Hl_3(1,1)} + C_{Hl_3(2,2)}) \right. \\ & + 0.252418 C_{Hq_3(1,1)} - 0.0029(C_{ll(1,1,2,2)} + C_{ll(2,2,1,1)}) \\ & + 0.001(C_{ll(1,2,2,1)} + C_{ll(2,1,1,2)}) + 0.463 C_{HD} + 0.0449 C_{HWB\bar{g}} \Big) \\ & - 0.0025(C_{Hl_1(1,1)} + C_{Hl_1(2,2)}) + 0.0473(C_{Hl_3(1,1)} + C_{Hl_3(2,2)}) \\ & + 1.0119 C_{Hq_3(1,1)} - 0.0206(C_{ll(1,1,2,2)} + C_{ll(2,2,1,1)}) \\ & + 0.0067(C_{ll(1,2,2,1)} + C_{ll(2,1,1,2)}) + 2.0729 C_{HD} + 0.3125 C_{HWB\bar{g}}, \end{aligned} \quad (37)$$

where μ_W is the scale of the matching which has been set to 2 GeV in our analysis. Note that the Standard Model has only left handed currents, and hence $L^{V,LR}$ is generated by new physics beyond the cut-off scale Λ and is, at best $O(\frac{v^2}{\Lambda^2})$. Thus to $O(\frac{v^2}{\Lambda^2})$, the $(L^{V,LR})^2$ term in the differential width may be neglected. On the other hand, for the two terms in Eq. 35 electron helicities are opposite. This implies that the interference between the two amplitudes would suffer an additional suppression by a factor (m_e/m_μ) or smaller. Even then, if we look at the tree and 1-loop matching of $L_{\nu e}^{V,LR}$ operator with the SMEFT Lagrangian, it consists of only $C_{le(2,1,1,2)}$ operator, which does not appear in EWPO and hence cannot be constrained. Thus we assume that this SMEFT operator vanishes and neglect the corresponding LEFT operator in further analysis.

This means that,

$$L_{\nu e}^{V,LL} = L_{\nu e \text{ tree}}^{V,LL} + L_{\nu e \text{ 1-loop}}^{V,LL} = -\frac{4G_F}{\sqrt{2}}, \quad (38)$$

4.2 Beta Decay

The low-energy effective Lagrangian for the process $d \rightarrow ue^- \bar{\nu}_e$ is given by,

$$\begin{aligned} \mathcal{L}_n = & L_{\nu edu}^{V,LL} (\bar{\nu}_L \gamma^\mu e_L) (\bar{u}_L \gamma_\mu d_L) + L_{\nu edu}^{V,LR} (\bar{\nu}_L \gamma^\mu e_L) (\bar{u}_R \gamma_\mu d_R) + L_{\nu edu}^{S,RR} (\bar{\nu}_L e_R) (\bar{u}_L d_R) \\ & + L_{\nu edu}^{S,RL} (\bar{\nu}_L e_R) (\bar{u}_L \gamma_\mu d_R) + L_{\nu edu}^{T,RR} (\bar{\nu}_L \sigma^{\mu\nu} e_R) (\bar{u}_L \sigma^{\mu\nu} d_R) \end{aligned} \quad (39)$$

where $L_{\nu edu}^{V,LL}, L_{\nu edu}^{V,LR}, L_{\nu edu}^{S,RR}, L_{\nu edu}^{S,RL}, L_{\nu edu}^{T,RR}$ are the LEFT WCs.

At tree level, the matching of the above Lagrangian with the SMEFT one gives,

$$L_{\nu edu \text{ tree}}^{V,LL} = \left(-\frac{2}{v^2} - 2(C_{Hl_3(1,1)} + C_{Hq_3(1,1)}) \right) U_{(1,1)}^\dagger V_{(1,1)}^\dagger \quad (40)$$

where V is the CKM matrix. Matching this Lagrangian with the SMEFT Lagrangian, at 1-loop, level we get,

$$\begin{aligned}
L_{\nu edu}^{V,LL} \text{ 1-loop} &= U_{11}^\dagger V_{11}^\dagger \left((0.0241 \log \mu_W^2 + 0.0595) C_{Hl_3(1,1)} \right. \\
&- (0.0139 \log \mu_W^2 + 0.0712) C_{Hq_1(1,1)} + (0.1007 \log \mu_W^2 \\
&+ 0.3931) C_{Hq_3(1,1)} + (0.1338 \log \mu_W^2 + 0.592) C_{HD} \\
&- \left. (0.0115 \log \mu_W^2 + 0.0715) C_{HWB\overline{g_1}} + 0.0007 C_{Hl_1(1,1)} \right).
\end{aligned} \tag{41}$$

The contribution from $L_{\nu edu}^{V,LR}$, $L_{\nu edu}^{S,RR}$ and $L_{\nu edu}^{T,RR}$ do not contain any SMEFT coefficients that contribute to the EWPO. Then, up to 1-loop order,

$$L_{\nu edu}^{V,LL} = L_{\nu edu}^{V,LL} \text{ tree} + L_{\nu edu}^{V,LL} \text{ 1-loop} = \frac{4G_F}{\sqrt{2}} V_{ud}^{eff}. \tag{42}$$

Using Eq.38, we get

$$\begin{aligned}
V_{ud}^{eff} = \frac{L_{\nu edu}^{V,LL}}{L_{\nu e}^{V,LL}} &= \frac{L_{\nu edu}^{V,LL} \text{ tree} + L_{\nu edu}^{V,LL} \text{ 1-loop}}{L_{\nu e}^{V,LL} \text{ tree} + L_{\nu e}^{V,LL} \text{ 1-loop}} \\
&= V_{11} (1 + \delta_{SMEFT} \text{ tree} + \delta_{SMEFT} \text{ 1-loop}),
\end{aligned} \tag{43}$$

$$\Delta_{CKM} = \delta_{SMEFT} \text{ tree} + \delta_{SMEFT} \text{ 1-loop}, \tag{44}$$

where

$$\begin{aligned}
\delta_{SMEFT} \text{ tree} &= 2(C_{Hl_3(1,1)} + C_{Hq_3(1,1)}) \\
&+ (-2C_{Hl_3(2,2)} + C_{ll(1,2,2,1)} + C_{ll(2,1,1,2)} - 2C_{Hl_3(1,1)}), \\
\delta_{SMEFT} \text{ 1-loop} &= -0.0029 C_{Hl_1(1,1)} - (0.0026 \log \mu_W^2 + 0.0172) C_{Hl_3(1,1)} \\
&+ (0.0139 \log \mu_W^2 + 0.0711) C_{Hq_1(1,1)} \\
&- (0.0255 \log \mu_W^2 + 0.0917) C_{Hq_3(1,1)} \\
&+ (0.004 \log \mu_W^2 + 0.0252) C_{HD} \\
&+ (0.0249 \log \mu_W^2 + 0.1645) C_{HWB\overline{g_1}},
\end{aligned} \tag{45}$$

Assuming flavor universal scenarios and removing indices, the contributions to SMEFT can be written as:

$$\begin{aligned}
\delta_{SMEFT} \text{ tree} &= 2(C_{Hl_3} + C_{Hq_3}) \\
&+ (-2C_{Hl_3} + C_{ll} + C_{ll} - 2C_{Hl_3}) \\
&= (2C_{ll} - 2C_{Hl_3} + 2C_{Hq_3}), \\
\delta_{SMEFT} \text{ 1-loop} &= -0.0029 C_{Hl_1} - (0.0026 \log \mu_W^2 + 0.0172) C_{Hl_3} \\
&+ (0.0139 \log \mu_W^2 + 0.0711) C_{Hq_1} \\
&- (0.0255 \log \mu_W^2 + 0.0917) C_{Hq_3} \\
&+ (0.004 \log \mu_W^2 + 0.0252) C_{HD} \\
&+ (0.0249 \log \mu_W^2 + 0.1645) C_{HWB\overline{g_1}},
\end{aligned} \tag{46}$$

Note that $V_{ud}^{eff} = V_{11}$ in the limit where all the SMEFT coefficients vanish and the tree-level result matches with [76].

5 Fitting procedure

The results of the fit involving the EWPO have a strong dependence on the input scheme [29]. In our analyses, we choose the $(G_F, M_Z$ and $\alpha)$ scheme and the input parameters we used are as follows:

$$\begin{aligned} G_F &= 1.1663787(6) \times 10^{-5} \text{ GeV}^{-2} \\ M_Z &= 91.1876 \pm .0021 \text{ GeV} \\ \frac{1}{\alpha_e} &= 137.035999139(31) \end{aligned} \tag{47}$$

Let the contribution of the higher dimensional SMEFT operators, along with SM, to the electroweak observables be represented as,

$$\mathcal{O}_i^{SMEFT} = \mathcal{O}_i^{SM} + \delta\mathcal{O}_i^{SMEFT}, \tag{48}$$

where $\delta\mathcal{O}_i^{SMEFT}$'s are the functions of WCs C_i 's. For \mathcal{O}_i^{SM} in Eq. 48, we list, in Table 3, the most

Measurement	Experiment	Precise Theory	Pull
$\Gamma_Z(\text{GeV})$	2.4955 ± 0.0023	2.4945 ± 0.0006	0.42
$\sigma_h(\text{nb})$	41.481 ± 0.033	41.482 ± 0.008	-0.29
R_l	20.767 ± 0.025	20.749 ± 0.009	0.67
R_b	0.21629 ± 0.00066	0.21582 ± 0.00002	0.71
R_c	0.1721 ± 0.0030	0.17221 ± 0.00003	-0.03
R_{uc}	0.166 ± 0.009	0.172227 ± 0.000032	-0.69
A_l	0.1465 ± 0.0033	0.1468 ± 0.0003	-0.09
$A_l(SLD)$	0.1513 ± 0.0021	0.1468 ± 0.0003	2.12
A_b	0.923 ± 0.020	0.92699 ± 0.00006	-0.19
A_c	0.670 ± 0.027	0.6677 ± 0.0001	0.08
A_s	0.895 ± 0.020	0.9356 ± 0.00004	-0.44
$A_{l,FB}$	0.0171 ± 0.0010	0.01617 ± 0.00007	0.92
$A_{b,FB}$	0.0996 ± 0.0016	0.1029 ± 0.0002	-2.04
$A_{c,FB}$	0.0707 ± 0.0035	0.0735 ± 0.0002	-0.79
$M_W(\text{GeV})$	80.4133 ± 0.008	80.360 ± 0.006	5.33
$\Gamma_W(\text{GeV})$	2.085 ± 0.042	2.0904 ± 0.0003	-0.13
$BR_{W \rightarrow \nu l}$	0.1086 ± 0.0009	0.108271 ± 0.000024	0.36
Δ_{CKM}	-0.0015 ± 0.0007	0 ± 0	-2.14

Table 3: Experimental and theoretical values and uncertainties of the observables. Pulls of the measurement with best theory is also provided in the last column [24, 31, 38, 79].

precisely calculated values. The form of the χ^2 is given by

$$\chi^2 = \sum_{i,j} (\mathcal{O}_i^{exp} - \mathcal{O}_i^{SMEFT}) \sigma_{ij}^{-2} (\mathcal{O}_j^{exp} - \mathcal{O}_j^{SMEFT}). \tag{49}$$

where the covariance matrix $\sigma_{ij}^2 = \Delta_i^{exp} \rho_{ij}^{exp} \Delta_j^{exp} + \Delta_i^{th} \rho_{ij}^{th} \Delta_j^{th}$. Here ρ_{ij}^{exp} is the experimental correlation matrix obtained from [19] and ρ_{ij}^{th} is identity. Δ_i^{exp} and Δ_i^{th} are the experimental and theory errors of the i^{th} observable. Inclusion of theoretical uncertainties and the correlations among the observables lead to better constraints over the parameters of interest.

In Table 3, we summarize the current status of the SM theory and the experimental results, including Δ_{CKM} . First we compute the χ^2 including the relevant observables from Table 3, thereby making it a

function of the WCs which we are interested in including in our fit. The χ^2 function is then minimized to get the best-fit values of the WCs. The 1σ ranges of the WCs are calculated by marginalizing over the other parameters. This is done in the following way: for the 1σ range of a parameter c_i of our interest, we define a partial χ^2 as follows.

$$\chi_{par}^2 = \chi_{c_i=x_0, c_j}^2 = \chi^2(x_0, c_j),$$

where x_0 is a random value for the variable c_i . c_j s are the other parameters present in the χ^2 over which the marginalization is performed. We then define the following test-statistic which is a difference between the minima of the partial χ^2 and the minima of the total χ^2

$$\min(\chi_{par}^2) - \min(\chi^2(c_i, c_j))$$

For each random value of c_i , we get some value for this new test-statistic, which can be used to obtain an interpolating function for c_i . The marginalized result for the 1σ spread of c_i is then obtained by demanding the value of the obtained interpolating function to be smaller than the 1σ value of the χ^2 function for a single variable.

The correlation between two WCs of our interest affecting the fit can also be calculated in a similar way by constructing a partial χ^2 for the two WCs and then obtaining their interpolating function through the test-statistic.

5.1 S, T, V fitting

The effects of new heavy particles (with mass M_{new}) on the gauge boson self-energies can be described by three parameters S , T , and U . The U parameter is not very sensitive to heavy New Physics because of the presence of an extra factor of M_Z/M_{new} and hence can be neglected. This S and T parametrisation can be mapped to the SMEFT WCs C_{HD} and C_{HWB} and has been studied in literature [80–83]. Along with them, we append the V parameter which parametrises the change in G_F . This parameter is crucial if we have to make the quarks and leptons interact with BSM resonances. As shown in Eq. 6, this shift in G_F can be mapped to the combination $2C_{Hl3} - C_U$. The expressions for the Electroweak Observables in terms of this S , T and V parametrisation are given in Table 4. For Δ_{CKM} , we infer the result by considering only the tree-level matching, where the dependence on V comes from the muon decay parameters sitting in the denominator of Eq 43. As can be seen from Table 4, this V parameter is very crucial for M_W as it has the highest sensitivity to this parameter, which can be inferred from its largish coefficient of V compared to other observables.

In Figure 1, we have plotted the change in S , T and V parameters with EWPO data and EWPO + Δ_{CKM} data in a 2-D plane by marginalising over the third parameter. Note that the inclusion of Δ_{CKM} constrains the Peskin-Takeuchi (S, T) parameters better in comparison with just the EWPO data. The results of the fit are presented in Table 5. The posterior values of the observables after the (S, T, V) can be read off from Table 6. Even without including the Δ_{CKM} constraint, we can see that this parametrisation has very good agreement with the experimental results of M_W and Δ_{CKM} simultaneously. The discrepancy in A_l^{SLD} and A_b^{FB} also moves below 2σ , thereby making this a parametrisation worth considering to look for BSM physics. Inclusion of Δ_{CKM} in the fit improves its agreement with the measured value, while slightly deteriorating A_l^{SLD} and A_b^{FB} .

Observables	Expression (S, T, V)
Γ_Z	$\Gamma_Z^{\text{SM}} - 0.0091 \Delta S + 0.0241 \Delta T - 3.3106 \Delta V$
σ_h	$\sigma_h^{\text{SM}} - 0.0471 \Delta S + 0.0315 \Delta T - 4.3194 \Delta V$
R_e	$R_e^{\text{SM}} - 0.0202 \Delta S + 0.0135 \Delta T - 1.8526 \Delta V$
R_b	$R_b^{\text{SM}} + 0.0001 \Delta S - 0.0001 \Delta T + 0.0149 \Delta V$
R_c	$R_c^{\text{SM}} - 0.0002 \Delta S + 0.0002 \Delta T - 0.0224 \Delta V$
A_l	$A_l^{\text{SM}} - 0.0237 \Delta S + 0.0158 \Delta T - 2.1688 \Delta V$
A_b	$A_b^{\text{SM}} - 0.0018 \Delta S + 0.0012 \Delta T - 0.1639 \Delta V$
A_c	$A_c^{\text{SM}} - 0.0097 \Delta S + 0.0065 \Delta T - 0.8894 \Delta V$
A_e^{FB}	$A_{e\text{FB}}^{\text{SM}} - 0.0105 \Delta S + 0.007 \Delta T - 0.9629 \Delta V$
A_b^{FB}	$A_{b\text{FB}}^{\text{SM}} - 0.0172 \Delta S + 0.0115 \Delta T - 1.5771 \Delta V$
A_c^{FB}	$A_{c\text{FB}}^{\text{SM}} - 0.0151 \Delta S + 0.0101 \Delta T - 1.3861 \Delta V$
M_W	$M_W^{\text{SM}} - 0.2565 \Delta S + 0.4041 \Delta T - 14.9135 \Delta V$
Γ_w	$\Gamma_w^{\text{SM}} - 0.0198 \Delta S + 0.0313 \Delta T - 3.2422 \Delta V$
$\text{Br}_{W \rightarrow \nu l}$	$\text{Br}_{W \rightarrow \nu l}^{\text{SM}} + 0.0007 \Delta S - 0.0011 \Delta T + 0.0407 \Delta V$
Δ_{CKM}	$-\Delta V$

Table 4: Expressions for observables in terms of ΔS , ΔT and ΔV .

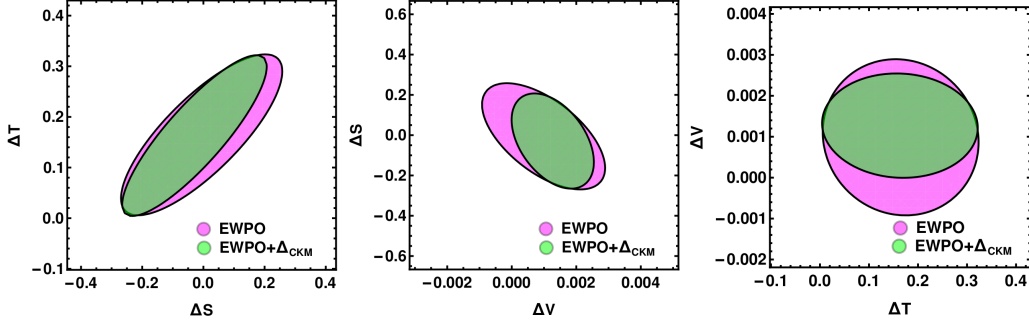


Figure 1: S, T and V parameters with EWPO and EWPO + Δ_{CKM} data

5.2 Study of C_{Hl_3} and C_u

As already seen from the expression of the recent anomalies in terms of SMEFT WCs, all tree-level C_{Hl_3} and C_u are the ones which are common both in M_W and Δ_{CKM} (using 1-loop matching result of Δ_{CKM}). Incidentally, these WCs are also the ones which affect the weak coupling constant G_F . However, along with changing a G_F , there is an additional dependence on the WC C_{Hl_3} coming from the shift in couplings for the observables as shown in Table 2. Similar to the (S, T, V) fit, we present two distinct cases, where first we have shown the fit to the EWPO. We then augment the number of observables by including Δ_{CKM} and then present the corresponding pulls of the observables after

WC	B.F(EWPO)	Correlation			B.F(EWPO+CKM)	Correlation		
	$(\chi^2_{\text{fit}}/\chi^2_{\text{SM}} = 11.41/40.08)$				$(\chi^2_{\text{fit}}/\chi^2_{\text{SM}} = 11.68/44.67)$			
ΔS	-0.0032 ± 0.1077	1.00			-0.0292 ± 0.0965	1.00		
ΔT	0.1646 ± 0.0649	0.79	1.00		0.1631 ± 0.06484	0.86	1.00	
ΔV	-0.001 ± 0.0007	-0.59	-0.07	1.00	0.0013 ± 0.0005	-0.44	-0.04	1.00

Table 5: Global fit of (S,T,V) parametrisation tree-level to EWPO and Δ_{CKM} .

Observables	Posterior(EWPO)	Pull	Posterior(EWPO+ Δ_{CKM})	Pull
Γ_Z	2.4953 ± 0.0019	0.05	2.4945 ± 0.001	0.39
σ_h	41.4832 ± 0.0064	-0.07	41.483 ± 0.0047	-0.06
R_e	20.7495 ± 0.0027	0.69	20.7494 ± 0.002	0.7
R_b	0.2158 ± 0.00002	0.72	0.2158 ± 0.00002	0.72
R_c	0.1722 ± 0.00003	-0.04	0.1722 ± 0.00003	-0.04
R_{uc}	0.1722 ± 0.00003	-0.69	0.1722 ± 0.00002	-0.69
A_l	0.1474 ± 0.0032	-0.19	0.1473 ± 0.0024	-0.19
A_l^{SLD}	0.1474 ± 0.0032	1.01	0.1473 ± 0.0024	1.26
A_b	0.927 ± 0.0002	-0.2	0.927 ± 0.0002	-0.2
A_c	0.6679 ± 0.0013	0.07	0.6679 ± 0.0009	0.08
A_s	0.9356 ± 0.0002	-0.45	0.9356 ± 0.0002	-0.45
A_e^{FB}	0.0164 ± 0.0014	0.38	0.0164 ± 0.0011	0.48
A_b^{FB}	0.1033 ± 0.0023	-1.32	0.1032 ± 0.0017	-1.56
A_c^{FB}	0.0739 ± 0.0021	-0.78	0.0738 ± 0.0015	-0.82
M_W	80.4131 ± 0.013	0.01	80.4143 ± 0.0062	-0.09
Γ_W	2.0925 ± 0.0026	-0.18	2.0919 ± 0.0016	-0.16
$\text{Br}_{W \rightarrow \nu l}$	0.1081 ± 0.00004	0.53	0.1081 ± 0.00002	0.53
Δ_{CKM}	-0.00096 ± 0.00078	-0.52	-0.00126 ± 0.00051	-0.27

Table 6: Observables posteriors using STV fit.

each step. As seen from Figure 2, the inclusion of Δ_{CKM} has a more constraining effect on the two

WC	B.F(EWPO)	Correlation		B.F(EWPO+CKM)	Correlation	
	$(\chi^2_{\text{fit}}/\chi^2_{\text{SM}} = 24.27/40.08)$			$(\chi^2_{\text{fit}}/\chi^2_{\text{SM}} = 105.36/126.37)$		
C_{Hl_3}	-0.0138 ± 0.0065	1.00		-0.0152 ± 0.0058	1.00	
C_u	-0.0008 ± 0.0114	0.86	1.00	-0.0034 ± 0.0084	0.88	1.00

Table 7: Global fit of the WCs common to W -mass and Δ_{CKM} (using 1-loop matching result of Δ_{CKM}).

WCs. Table 7 presents the result of the fit and correlation among the WCs. The posterior results for the observables are given in Table 8. For the first case with only the EWPO observables in the fit, the discrepancy in M_W comes down to 2.85σ . The discrepancy in A_b^{FB} however deteriorates to -2.9σ . Discrepancy in Δ_{CKM} however comes down to a mere 0.14σ . Inclusion of the Δ_{CKM} constraint in the fit does not significant constrain it. Thus one can argue that any New Physics effect coming through these two parameters (or δG_F) cannot fully satisfy the EWPO data. This also strengthens the case

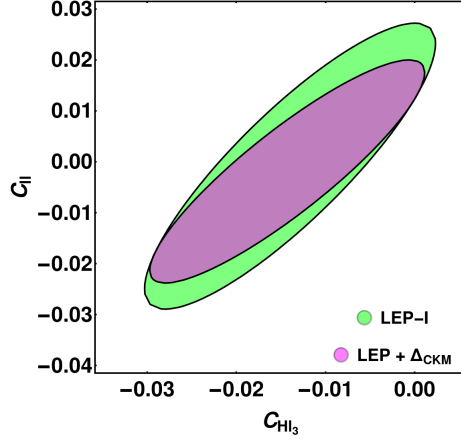


Figure 2: Marginalised 2-D plot for WCs common to W -mass and Δ_{CKM} .

Observables	Posterior(EWPO)	Pull	Posterior(EWPO+ Δ_{CKM})	Pull
Γ_Z	2.4986 ± 0.0012	-1.2	2.4985 ± 0.0009	-1.2
σ_h	41.454 ± 0.0158	0.74	41.453 ± 0.0146	0.77
R_e	20.7907 ± 0.0188	-0.76	20.7917 ± 0.0179	-0.8
R_b	0.2158 ± 0.00001	0.75	0.2158 ± 0.00001	0.75
R_c	0.1722 ± 0.00001	-0.05	0.1722 ± 0.00001	-0.05
R_{uc}	0.1723 ± 0.00001	-0.69	0.1723 ± 0.00001	-0.69
A_l	0.149 ± 0.0008	-0.74	0.1489 ± 0.0005	-0.73
A_l^{SLD}	0.149 ± 0.0008	1.01	0.1489 ± 0.0005	1.08
A_b	0.9273 ± 0.00007	-0.21	0.9272 ± 0.00006	-0.21
A_c	0.6692 ± 0.0004	0.03	0.6691 ± 0.0003	0.03
A_s	0.9359 ± 0.00007	-0.45	0.9359 ± 0.00006	-0.45
A_e^{FB}	0.0171 ± 0.0003	-0.05	0.0171 ± 0.0002	-0.02
A_b^{FB}	0.1045 ± 0.0006	-2.9	0.1045 ± 0.0004	-2.96
A_c^{FB}	0.075 ± 0.0005	-1.23	0.0749 ± 0.0003	-1.22
M_W	80.3845 ± 0.0062	2.85	80.3842 ± 0.0057	2.97
Γ_w	2.0945 ± 0.0012	-0.23	2.0944 ± 0.0009	-0.22
$Br_{W \rightarrow \nu l}$	0.1081 ± 0.00007	0.58	0.1081 ± 0.00006	0.58
Δ_{CKM}	-0.00165 ± 0.0008	0.14	-0.00156 ± 0.00052	0.08

Table 8: Posterior results and Pull for WCs common to M_W and Δ_{CKM} , once just with EWPO observables and once including the Δ_{CKM} constraint.

for the (S, T, V) parametrisation, where presence of extra parameters S and T (or equivalently C_{HD} and C_{HWB}) help us explain all the observables within 2σ discrepancy.

5.3 Study of C_{HD} , C_{HWB} , C_{Hl_3} and C_l

With the result from CDF impacting the world-average of W-mass, the discrepancy now stands at around 5.3σ from the SM value. Taking it as a sign of BSM physics, we look at a fit with just the SMEFT operators contributing to W-mass at tree-level. The shift in W mass in SMEFT can be written as:

$$\frac{\delta M_W^2}{M_W^2} = v^2 \frac{s_W c_W}{s_W^2 - c_W^2} \left[2C_{HWB} + \frac{c_W}{2s_W} C_{HD} + \frac{s_W}{c_W} (2C_{Hl}^{(3)} - C_l) \right], \quad (50)$$

This can also be thought of as augmenting the previous fit by including two more parameters C_{HD} and C_{HWB} . The results of the fit and the 2-D marginalised plots are shown in Table 9 and Figure 3. The plot here shows that the inclusion of the Δ_{CKM} constraint (matched to SMEFT at 1-loop level) has significant impact on the results of the fit with C_{HWB} and C_l seeing noticeable shifts in their best fit points and their 2σ reaches. The correlations among the WCs also show significant changes, with the C_l - C_{HWB} and C_l - C_{Hl_3} pairs showing the highest change.

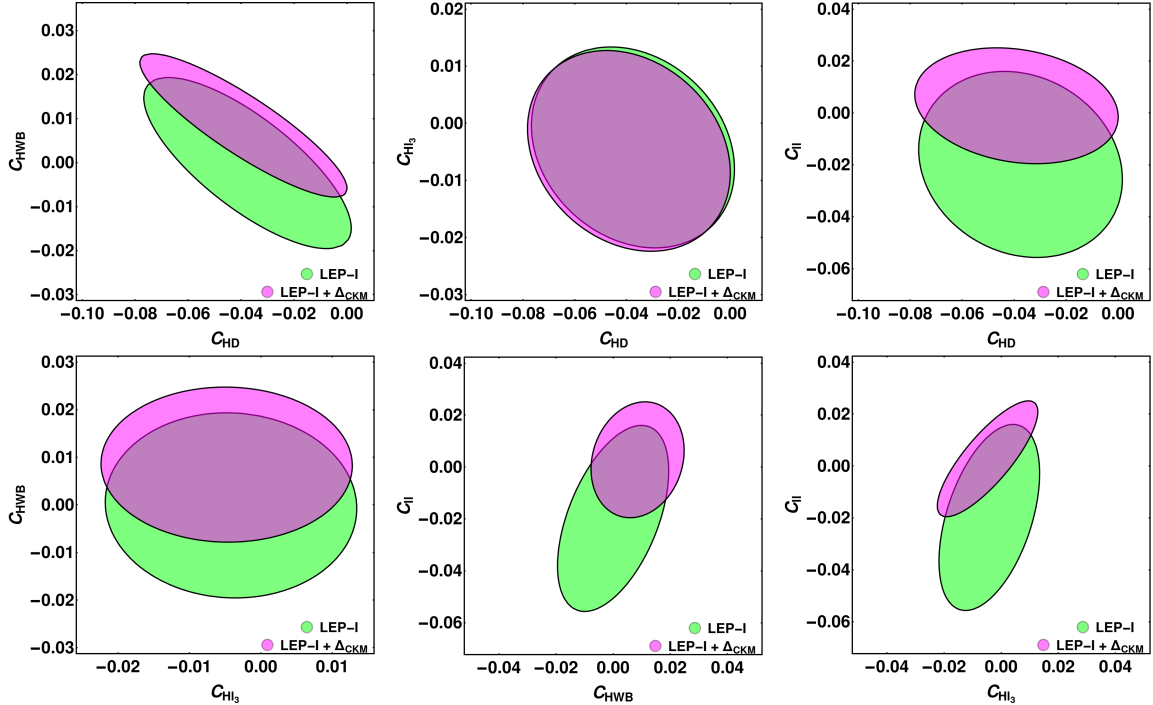


Figure 3: 2-D marginalised global fit of the four WCs affecting M_W at tree level.

WC	B.F(EWPO)	Correlation					B.F(EWPO+CKM)	Correlation				
		$(\chi_{\text{fit}}^2/\chi_{\text{SM}}^2 = 11.07/40.08)$						$(\chi_{\text{fit}}^2/\chi_{\text{SM}}^2 = 14.96/44.67)$				
C_{HD}	-0.0376 ± 0.0159	1.00					-0.0392 ± 0.0159	1.00				
C_{HWB}	-0.00007 ± 0.0079	-0.76	1.00				0.0085 ± 0.0066	-0.87	1.00			
C_{Hl_3}	-0.0042 ± 0.0072	-0.21	-0.04	1.00			-0.0048 ± 0.0072	-0.21	-0.01	1.00		
C_l	-0.0198 ± 0.0146	-0.15	0.51	0.47	1.00		0.0028 ± 0.0091	-0.19	0.16	0.81	1.00	

Table 9: Global fit of the WCs affecting the W-boson mass at tree-level

The posterior values for the observables are given in Table 10. For the fit with EWPO, the discrepancy in M_W , as expected, is drastically reduced. A_l^{SLD} also comes down under 2σ . However A_b^{FB} and Δ_{CKM} shows the highest discrepancy with a deviation of -2.09σ and -1.97σ respectively. Inclusion of the

Observables	Posterior(EWPO)	Pull	Posterior(EWPO+ Δ_{CKM})	Pull
Γ_Z	2.4956 ± 0.0023	-0.03	2.4994 ± 0.0012	-1.49
σ_h	41.4734 ± 0.0169	0.2	41.4728 ± 0.0168	0.22
R_e	20.7615 ± 0.0204	0.17	20.7636 ± 0.0204	0.1
R_b	0.2158 ± 0.00001	0.72	0.2158 ± 0.00001	0.73
R_c	0.1722 ± 0.00001	-0.04	0.1722 ± 0.00001	-0.04
R_{uc}	0.1722 ± 0.00001	-0.69	0.1722 ± 0.00001	-0.69
A_l	0.1474 ± 0.0011	-0.26	0.1478 ± 0.0011	-0.38
A_l^{SLD}	0.1474 ± 0.0011	1.63	0.1478 ± 0.0011	1.45
A_b	0.927 ± 0.0001	-0.2	0.9271 ± 0.0001	-0.2
A_c	0.6681 ± 0.0005	0.07	0.6683 ± 0.0005	0.06
A_s	0.9357 ± 0.0001	-0.45	0.9357 ± 0.0001	-0.45
A_e^{FB}	0.0164 ± 0.0005	0.59	0.0166 ± 0.0005	0.42
A_b^{FB}	0.1033 ± 0.0008	-2.07	0.1036 ± 0.0008	-2.24
A_c^{FB}	0.0739 ± 0.0007	-0.89	0.0742 ± 0.0007	-0.98
M_W	80.4131 ± 0.0097	0.02	80.4074 ± 0.0097	0.46
Γ_w	2.0927 ± 0.0016	-0.18	2.0952 ± 0.0009	-0.24
$Br_{W \rightarrow \nu l}$	0.108 ± 0.00007	0.57	0.1081 ± 0.0001	0.56
Δ_{CKM}	0.0019 ± 0.0015	-1.97	-0.00093 ± 0.00063	-0.59

Table 10: Posterior results and Pull for WCs effecting M_W , once just with EWPO observables and once including the Δ_{CKM} constraint.

Δ_{CKM} constraint along with EWPO reduces its discrepancy significantly to -0.59σ at the expense of worsening A_b^{FB} to -2.24σ . The agreement of Γ_Z also suffers with its discrepancy increasing from -0.03σ to -1.49σ . This study thus indicates that we need to go beyond these four WCs in order to satisfy the precision data.

5.4 VLL inspired study

Inspired by various see-saw like scenarios that admit the possibility to address other shortcomings of the SM like muon ($g-2$), neutrino mass etc., we take a closer look at various Vectorlike leptons multiplets by identifying the leading dimension-6 operators which get affected. The list of leptons along with their corresponding Yukawa coupling λ_l (where l represents the corresponding vectorlike lepton) and the masses of the heavy states M_l are shown in Table 11. As seen from the table, the tree-level imprints of the model parameters on the SMEFT WCs are restricted to C_{He} , C_{Hl_1} and C_{Hl_3} .

Figure 4 and Table 12 represents the result of the fit once for the EWPO alone and second for the case including Δ_{CKM} (matched to SMEFT at 1-loop level) alongwith EWPO. The posterior values of the observables for these two cases can be read off from Table 13. We can see that even without including the Δ_{CKM} constraint, we can satisfy both M_W and Δ_{CKM} within 2σ . A_l^{SLD} improves to 1.56σ while A_B^{FB} deteriorates to -2.18σ . Inclusion of the Δ_{CKM} constraint improves the posterior

VLF	$(SU(2)_L, Y)$	Interaction	C_{He}	C_{Hl_1}	C_{Hl_3}
N^a	$(3, 0)$	$N^a(H\epsilon\tau^a L)$	0	$+\lambda_N^2/4M_N^2$	$-\lambda_N^2/4M_N^2$
N'	$(1, 0)$	$N' LH$	0	$+3\lambda_N^2/4M_N^2$	$+\lambda_N^2/4M_N^2$
L'	$(2, -1/2)$	$EL'H^*$	$-\lambda_L^2/2M_L^2$	0	0
$L_{3/2}$	$(2, -3/2)$	$E(L_{3/2}\epsilon H)$	$+\lambda_L^2/2M_L^2$	0	0
E'	$(1, 1)$	$E' LH^*$	0	$-\lambda_E^2/4M_E^2$	$-\lambda_E^2/4M_E^2$
E^a	$(3, 1)$	$E^a(H^*\tau^a L)$	0	$-3\lambda_E^2/4M_E^2$	$+\lambda_E^2/4M_E^2$

Table 11: List of new leptons that can couple to the SM lepton doublet $L = (\nu_\mu, l_L)$ or singlet $E = l_R$ (with the same gauge quantum numbers as L' and E') and to the Higgs doublet $H = (0, v + h/\sqrt{2})$ (an $SU(2)$ doublet with $Y = 1/2$).

value of Δ_{CKM} only marginally, while pushing the M_W value beyond 2σ . We can put limits on the

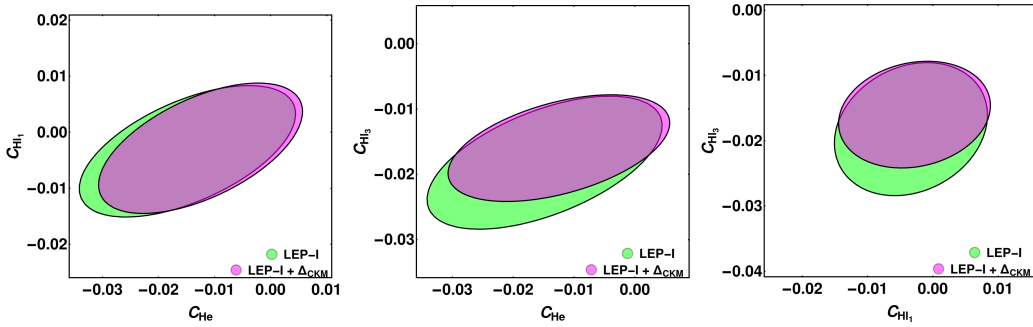


Figure 4: 2-D Marginalised plot for the WCs impacting the VLLs

WC	B.F(EWPO)	Correlation			B.F(EWPO+CKM)	Correlation		
	$(\chi_{\text{fit}}^2/\chi_{\text{SM}}^2=20.53/40.08)$				$(\chi_{\text{fit}}^2/\chi_{\text{SM}}^2=21.32/44.67)$			
C_{He}	-0.0148 ± 0.0075	1.00			-0.0125 ± 0.0073	1.00		
C_{Hl_1}	-0.0037 ± 0.0043	0.57	1.00		-0.0027 ± 0.0045	0.56	1.00	
C_{Hl_3}	-0.0184 ± 0.0039	0.55	0.21	1.00	-0.0158 ± 0.0027	0.47	0.17	1.00

Table 12: Global fit of the WCs affecting VLLs at tree-level to EWPO and Δ_{CKM} .

ratio of the coupling and mass for these scenarios. For example, if we consider only N' , we get a limit of $v\lambda_N/M_N < 0.074$, where v is the vev. Similarly for E' , we get a limit of $v\lambda_E/M_E < 0.05$. If we look at $L' \oplus E'$, the bounds come out to be $v\lambda_L/M_L < 0.045$ and $v\lambda_E/M_E < 0.066$.

5.5 EWPO and Δ_{CKM} : 8 parameter fit

Though, at leading order, EWPO depend on ten SMEFT operators, only eight among these can be constrained using the electroweak data. Some of the earlier literature [25, 38] redefined the combinations of the corresponding WCs by rotating away the two purely bosonic contributions (C_{HD} and C_{HWB}) to get eight independent parameters which are finally constrained. When analyzed in that fashion, we showed that our results are in well agreement with those in the literature. We also found out that same constraints can also be achieved by setting those two purely bosonic WCs just to zero. Slight variation of results in both our analyses do arise compared to previous analyses because of the choice of the input scheme and inclusion of theoretical uncertainties. Phenomenologically, there can

Observables	Posterior(EWPO)	Pull	Posterior(EWPO+ Δ_{CKM})	Pull
Γ_Z	2.5007 ± 0.0014	-1.91	2.4997 ± 0.0009	-1.71
σ_h	41.4707 ± 0.0241	0.25	41.4742 ± 0.0253	0.16
R_e	20.784 ± 0.0129	-0.6	20.7787 ± 0.0125	-0.42
R_b	0.2158 ± 0.00001	0.76	0.2158 ± 0.00001	0.75
R_c	0.1723 ± 0.00001	-0.05	0.1722 ± 0.00001	-0.05
R_{uc}	0.1723 ± 0.00001	-0.69	0.1723 ± 0.00001	-0.69
A_l	0.1476 ± 0.0011	-0.31	0.1476 ± 0.0011	-0.3
A_l^{SLD}	0.1476 ± 0.0011	1.57	0.1476 ± 0.0011	1.56
A_b	0.9274 ± 0.00008	-0.22	0.9273 ± 0.00005	-0.22
A_c	0.6697 ± 0.0004	0.01	0.6694 ± 0.0003	0.02
A_s	0.9359 ± 0.00008	-0.45	0.9359 ± 0.00005	-0.45
A_e^{FB}	0.01651 ± 0.0005	0.53	0.0165 ± 0.0005	0.53
A_b^{FB}	0.1035 ± 0.0008	-2.21	0.1035 ± 0.0008	-2.17
A_c^{FB}	0.0744 ± 0.0006	-1.03	0.0743 ± 0.0006	-1.01
M_W	80.3932 ± 0.0071	1.87	80.804 ± 0.00001	2.63
Γ_W	2.096 ± 0.0012	-0.26	$0.0021 \pm 1. \times 10^{-6}$	-0.24
$Br_{W \rightarrow \nu l}$	0.108 ± 0.00005	0.65	0.108 ± 0.00003	0.61
Δ_{CKM}	-0.0023 ± 0.0005	0.94	-0.0019 ± 0.0003	0.63

Table 13: Posterior results and Pull for the VLL inspired study, once just with EWPO observables and once including the Δ_{CKM} constraint.

be frameworks where these bosonic operators are highly suppressed and so this procedure can direct provide limits for such kind of scenarios.

The results of these analyses are presented in Table 14. The second column of the table shows the best fit and deviation for the WCs given in the first column. Deviations are computed using the marginalization procedure discussed in the section 5. We also tabulate the correlations between the coefficients in the last column. Among them, C_{Hl_3} and C_{ll} are highly correlated with a value of 0.94. The same for C_{Hl_1} and C_{ll} is 0.81 and for C_{Hl_1} and C_{Hl_3} it is -0.67 . From the shifts in the gauge coupling shown in Table 2, one can expect very small correlations among quark WCs and leptonic one $\sim \mathcal{O}(0.01)$. The value of the SMEFT χ^2 after the fit comes out to be 3.24 compared the SM χ^2 of 40.08, implying a very good quality of the fit. The 2-D marginalized distributions of the WCs are shown in Figure 5 in purple colour.

Posterior values of the EWPO observables show very good agreement with the experimental data with all of them within 1σ as shown in Table 16. Notable improvements among them are M_W at -0.2σ , A_b^{FB} at -0.19σ and A_l^{SLD} at 0.84σ . Δ_{CKM} however becomes worse as the pull with the EWPO fitted parameters increases its discrepancy to -2.7σ .

Inclusion of the CKM anomaly (Δ_{CKM} matched to SMEFT at 1-loop level), along with EWPO, shifts the best-fit values of the WCs, constraining them better. The results of the fit can be read off from Table 15 and the 2-D marginalized distributions of the WCs are given in Figure 5 in green colour. Δ_{CKM} has the largest dependence on C_{Hl_1} , C_{ll} , C_{Hl_3} and C_{Hq_3} ; therefore there is significant change

WC	B.F(EWPO)	Correlation								
		$(\chi^2_{\text{fit}}/\chi^2_{\text{SM}} = 3.24/40.08)$								
C_{Hd}	-0.4646 ± 0.1715	1.00								
C_{He}	-0.0099 ± 0.0085	-0.36	1.00							
C_{Hl_1}	-0.0031 ± 0.011	-0.12	0.42	1.00						
C_{Hl_3}	-0.0398 ± 0.0159	-0.05	0.08	-0.67	1.00					
C_{Hq_1}	0.0101 ± 0.0341	0.21	-0.08	0.01	-0.04	1.00				
C_{Hq_3}	-0.0989 ± 0.0310	0.59	-0.17	0.03	0.06	-0.42	1.00			
C_{Hu}	0.1162 ± 0.1195	-0.14	0.10	0.07	-0.03	0.44	-0.76	1.00		
C_{ll}	-0.0204 ± 0.0284	-0.06	-0.10	-0.81	0.94	-0.04	-0.03	-0.01	1.00	

Table 14: Global fit to EWPO for the case with 8 WCs.

WC	B.F(EWPO+ Δ_{CKM})	Correlation								
		$(\chi^2_{\text{fit}}/\chi^2_{\text{SM}} = 10.88/44.67)$								
C_{Hd}	-0.2125 ± 0.1453	1.00								
C_{He}	-0.0166 ± 0.0083	-0.24	1.00							
C_{Hl_1}	-0.0136 ± 0.0107	0.08	0.35	1.00						
C_{Hl_3}	-0.0238 ± 0.0148	-0.31	0.19	-0.63	1.00					
C_{Hq_1}	-0.0291 ± 0.0311	0.55	-0.23	-0.16	0.12	1.00				
C_{Hq_3}	-0.0221 ± 0.0139	0.30	0.18	0.78	-0.64	-0.13	1.00			
C_{Hu}	-0.1206 ± 0.0832	0.40	-0.15	-0.27	0.37	0.23	-0.37	1.00		
C_{ll}	0.0076 ± 0.0265	-0.32	0.01	-0.79	0.93	0.13	-0.83	0.38	1.00	

Table 15: Global fit to EWPO and Δ_{CKM} for the case with 8 WCs.

in the correlations involving these WCs. C_{Hq_3} and C_{ll} become highly correlated with a value of -0.83 . As Δ_{CKM} depends only on left chiral operators, the correlation of their WCs to that of the right chiral ones decrease. Δ_{CKM} also introduces a high correlation between the WCs corresponding to leptonic and quark operators, e.g., the correlation factor for C_{Hq_3} with C_{Hl_1} and C_{Hl_3} now stands at 0.78σ and -0.64σ respectively.

On the other hand, the inclusion of Δ_{CKM} in the fit observable reduces its discrepancy to a mere -0.32σ . However, discrepancy in A_c^{FB} , A_b^{FB} and A_l^{SLD} goes beyond 1σ . The other observables also show good agreement with the experimental observations.

5.6 Including LEP-II data to EWPO and Δ_{CKM} : 10 parameter fit

As discussed in the previous subsection, EWPO can only constrain eight of the 10 WCs. This can be overcome by including LEP-II data. During the second run of the LEP, sufficient energy was reached for the production of a pair of on-shell W bosons, dominant contribution coming from a t -channel neutrino exchange. This provides an opportunity to test four-fermionic final states at the collider. Precise measurements of cross-sections and angular distributions at various energies enhance the list of precision observables. Ref. [30, 36, 75] also explored this in the context of SMEFT and showed that the presence of the subdominant s -channel production of a pair of W bosons through a γ or Z exchange lifts up the flat directions which were there in the case of Z -pole EWPO. In addition to the 10 WCs already affecting the EWPO, introduction of LEP-II data brings dependence on the anomalous triple gauge operator [$\mathcal{O}_W \equiv W_\mu^\nu W_\nu^\rho W_\rho^\mu$] with the WC C_W (in the Warsaw basis) in the set of operators contributing at tree-level. As this is not part of EWPO or Δ_{CKM} we set $C_W = 0$ for our analyses.

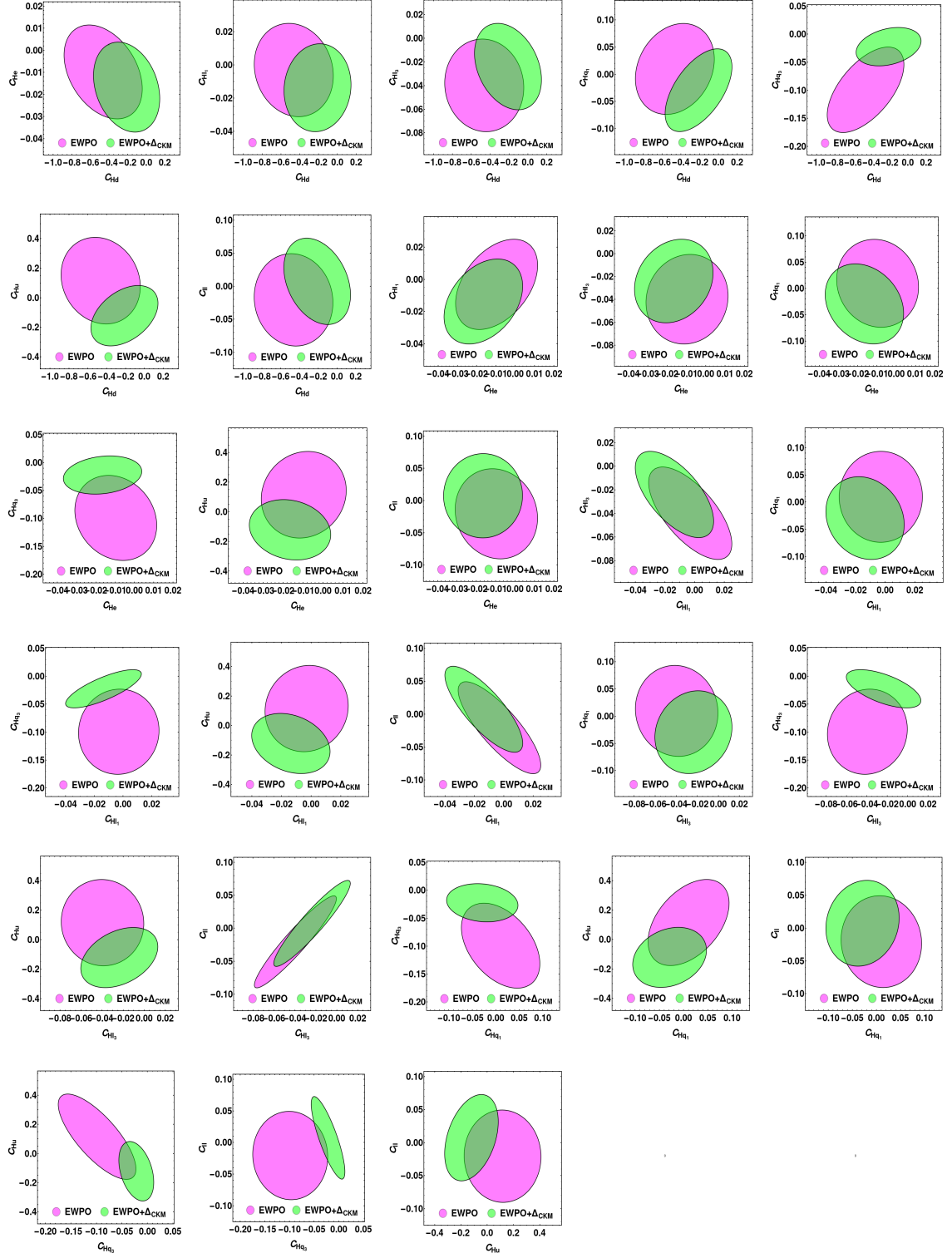


Figure 5: 2-D marginalised plot for the fit with 8 WCs

Observable	EWPO Posterior	Pull	Posterior (EWPO + Δ_{CKM})	Pull
Γ_Z	2.4955 ± 0.0023	-0.02	2.498 ± 0.0022	-0.81
σ_h	41.4822 ± 0.0316	-0.03	41.46 ± 0.031	0.45
R_e	20.7668 ± 0.0258	0.004	20.754 ± 0.025	0.36
R_b	0.2163 ± 0.0006	-0.05	0.216 ± 0.0006	0.26
R_c	0.1714 ± 0.0009	0.22	0.1719 ± 0.0009	0.07
R_{uc}	0.1714 ± 0.0009	-0.6	0.1719 ± 0.0009	-0.65
A_l	0.1492 ± 0.0013	-0.75	0.1483 ± 0.0013	-0.5
A_l^{SLD}	0.1492 ± 0.0013	0.84	0.1483 ± 0.0013	1.2
A_b	0.9064 ± 0.0077	0.77	0.9178 ± 0.0065	0.24
A_c	0.6549 ± 0.0135	0.49	0.683 ± 0.0089	-0.45
A_s	0.915 ± 0.0077	-0.21	0.9264 ± 0.0065	-0.34
A_e^{FB}	0.0172 ± 0.0006	-0.11	0.0168 ± 0.0006	0.22
A_b^{FB}	0.1 ± 0.0015	-0.19	0.1019 ± 0.0013	-1.1
A_c^{FB}	0.0719 ± 0.0029	-0.28	0.0777 ± 0.0021	-1.7
M_W	80.4136 ± 0.0099	-0.02	80.4099 ± 0.0098	0.26
Γ_w	2.0819 ± 0.0051	0.07	2.0955 ± 0.0015	-0.25
$Br_{W \rightarrow \nu l}$	0.1086 ± 0.0003	-0.06	0.1081 ± 0.0002	0.51
Δ_{CKM}	0.0096 ± 0.0039	-2.7	0.0012 ± 0.0007	-0.32

Table 16: Posterior Value and Pulls for the EWPO observables with 8 WCs, once without Δ_{CKM} and once with Δ_{CKM}

Including the LEP-II data increases the χ^2 to 121 due to the increase in number of observables. The results of the fit without including Δ_{CKM} are shown in the Table 17. The minimum value of χ^2 now decreases to 83.8. But, the best fit values of C_{HD} , C_{HWB} and C_{He} are slightly on the larger side. The correlations among the WCs change drastically due to the presence of the new LEP-II observables. Correlation between C_{Hl_3} and C_l becomes almost negligible while many pairs of WCs become highly correlated. To show the strength of correlation we also plot color density matrix plot in Figure 6(a). Highest correlation is represented by darkish blue colour and gradually turns towards green as strength of the correlation decreases. It can be easily observed that many of them are dark blue with correlation ~ 0.9 . The correlation of all WCs with C_l is small ~ 0.3 and almost no correlation with C_{Hl_3} and C_{Hq_3} . The correlation of C_{Hl_3} and C_{Hq_3} is almost 1 whereas both of them are less correlated with others. The posterior results of the fit for the precision observables are shown in Table 19. The discrepancy in all of these observables are within 1σ with the exception of Δ_{CKM} where the pull for is -2.7σ .

Incorporation of Δ_{CKM} (matched to SMEFT at 1-loop level) as an observable in the fit makes it more constraining as shown in Table 18. The absolute best-fit values of the WCs lie well within 1 with C_l becoming very small. There is no significant change found in 1σ deviations of WCs and the correlations among the pairs of WCs also do not show much change. The density plot for correlation matrix assuming magnitude of elements is also shown in Figure 6(b).

	Result	Correlation									
		$(\chi^2_{\text{Fit}}/\chi^2_{\text{SM}} = 83.82/121.79)$									
C_{Hd}	-0.0841 ± 0.3937	1.00									
C_{HD}	-2.1541 ± 2.2945	-0.90	1.00								
C_{He}	1.0669 ± 1.1474	0.90	-0.99	1.00							
C_{Hl_1}	0.5383 ± 0.5713	0.90	-0.99	0.99	1.00						
C_{Hl_3}	0.01423 ± 0.4149	0.58	-0.60	0.60	0.61	1.00					
C_{Hq_1}	-0.1717 ± 0.1912	-0.87	0.98	-0.98	-0.98	-0.60	1.00				
C_{Hq_3}	-0.0346 ± 0.41	0.57	-0.58	0.58	0.58	0.99	-0.58	1.00			
C_{Hu}	-0.6179 ± 0.7532	-0.90	0.99	-0.99	-0.99	-0.61	0.98	-0.59	1.00		
C_{HWB}	1.0071 ± 0.9923	0.88	-0.98	0.98	0.98	0.46	-0.97	0.43	-0.97	1.00	
C_U	-0.0295 ± 0.0273	0.27	-0.29	0.29	0.27	0.005	-0.30	-0.028	-0.30	0.32	1.00

Table 17: Best fit with 1σ deviation of WCs after including LEP-II data along with EWPO. Correlation matrix of coefficients are also shown in the third column.

	Result	Correlation									
		$(\chi^2_{\text{Fit}}/\chi^2_{\text{SM}} = 90.93/126.37)$									
C_{Hd}	-0.1266 ± 0.3934	1.00									
C_{HD}	-0.5455 ± 2.2138	-0.93	1.00								
C_{He}	0.2564 ± 1.1066	0.93	-0.99	1.00							
C_{Hl_1}	0.125 ± 0.5498	0.93	-0.99	0.99	1.00						
C_{Hl_3}	-0.3029 ± 0.3974	0.59	-0.57	0.57	0.58	1.00					
C_{Hq_1}	-0.07295 ± 0.1876	-0.88	0.98	-0.99	-0.99	-0.58	1.00				
C_{Hq_3}	-0.2994 ± 0.403	0.57	-0.55	0.55	0.56	0.99	-0.56	1.00			
C_{Hu}	-0.2947 ± 0.7434	-0.90	0.99	-0.99	-0.99	-0.60	0.98	-0.58	1.00		
C_{HWB}	0.4054 ± 0.9663	0.90	-0.98	0.98	0.98	0.42	-0.97	0.39	-0.97	1.00	
C_U	-0.00004 ± 0.0249	0.31	-0.44	0.44	0.43	0.14	-0.42	0.08	-0.41	0.47	1.00

Table 18: Best fit with 1σ deviation of WCs after including LEP-II data along with EWPO and Δ_{CKM} . Correlation matrix of coefficients are also shown in the third column.

Posteriors results and pull of the EWPO and Δ_{CKM} are collected in the fourth column and fifth column respectively of Table 19. All the pulls are again within 1σ . As expected, pull for Δ_{CKM} improves to -0.36σ . The other observables continue to remain well within 1σ making the fit highly competitive with respect to the experimental data.

6 Summary and conclusions

Electroweak precision measurements place some of the most stringent constraints on all New Physics extensions of Standard Model. We explore dimension-6 operator subsets of the SMEFT in the context of Electroweak Precision data and the recent M_W anomaly with the latter hinting at the presence of BSM physics. In addition to the precision data, we also analyze the status of the Cabibbo anomaly within SMEFT using the most recent data. To implement it in a more precise way, we compute the contributions to the beta decay and muon decay using the SMEFT operators that enters in the LEFT at one loop matching. The results of this model-independent study are, then, used to investigate a few specific UV-complete BSM scenarios that are inspired by various anomalies in the experimental data.

To begin with, we parameterize the impact of BSM heavy states in oblique parameters S , T and V and compute the posterior fit of the EWPO and Δ_{CKM} . The results are impressive as pulls for almost all the observables (except A_l^{SLD} and A_b^{FB}) are within 1σ . Another point to note is that even without including Δ_{CKM} into the fit the pull for Cabibbo anomaly comes down to ~ -0.52 . On including Δ_{CKM} , the pull improves to ~ -0.27 . In the next study, we choose the SMEFT operators C_{Hl_3} and C_U as the ones which dictates the UV BSM physics as both of them affect the M_W , G_F and Δ_{CKM} at

Observable	Posterior(EWPO)	Pull	Posterior (EWPO+ Δ_{CKM})	Pull
Γ_Z	2.4952 ± 0.007	0.038	2.4976 ± 0.01451	-0.14
σ_h	41.4875 ± 0.1263	-0.049	41.4649 ± 0.0944	0.16
R_e	20.7731 ± 0.0565	-0.098	20.7588 ± 0.1351	0.06
R_b	0.2163 ± 0.0006	-0.025	0.216 ± 0.0006	0.24
R_c	0.1715 ± 0.0009	0.19	0.1718 ± 0.0009	0.08
R_{uc}	0.1715 ± 0.0009	-0.60	0.1718 ± 0.0009	-0.64
A_l	0.1491 ± 0.0086	-0.27	0.1483 ± 0.0138	-0.12
A_l^{SLD}	0.1491 ± 0.0086	0.25	0.1483 ± 0.0138	0.21
A_b	0.9074 ± 0.0077	0.72	0.9176 ± 0.0067	0.25
A_c	0.6569 ± 0.0135	0.43	0.6821 ± 0.0115	-0.41
A_s	0.916 ± 0.0077	-0.23	0.9262 ± 0.0067	-0.34
A_e^{FB}	0.0172 ± 0.0038	-0.019	0.0168 ± 0.0061	0.05
A_b^{FB}	0.1002 ± 0.0064	-0.085	0.1018 ± 0.0102	-0.21
A_c^{FB}	0.0723 ± 0.0061	-0.23	0.0775 ± 0.0094	-0.67
M_W	80.4144 ± 0.0862	-0.013	80.4106 ± 0.181	0.01
Γ_W	2.0826 ± 0.0112	0.054	2.0949 ± 0.0198	-0.21
$Br_{W \rightarrow \nu l}$	0.1085 ± 0.0005	0.039	0.1081 ± 0.0008	0.41
Δ_{CKM}	0.0096 ± 0.004	-2.7	-0.0012 ± 0.0005	-0.36

Table 19: Observable's posterior values for the all-parameter fit with 10 WCs

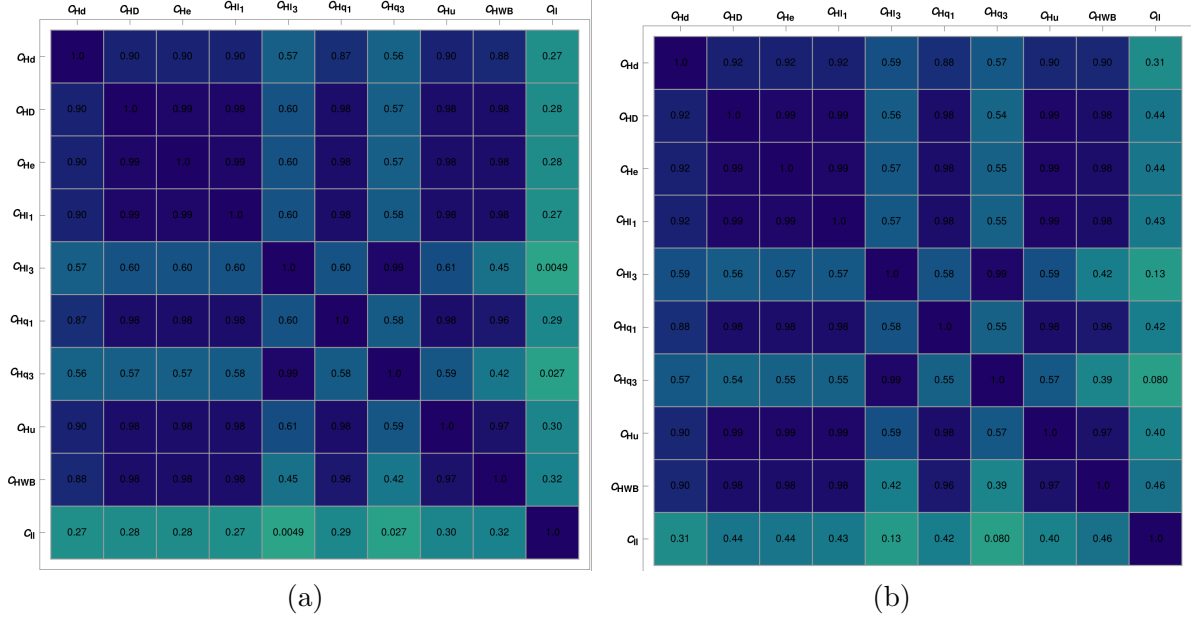


Figure 6: Density plot of correlation matrix after including LEP-II data: (a) EWPO (b) EWPO+ Δ_{CKM} .

tree level. We analyze this case for EWPO as well as the EWPO+ Δ_{CKM} (Δ_{CKM} matched to SMEFT

at 1-loop level) combination. Although they can explain the Cabibbo anomaly very well, they fare very badly with M_W and A_b^{FB} .

Since M_W has the highest pull away from the SM among the observables of our interest, we next considered the BSM case which consists of the four operators that affect the M_W at tree level (C_{HD} , C_{HWB} , C_{Hl_3} and C_U). The minimum value of χ^2 comes down to ~ 11 from ~ 40 and the fit fares very well with M_W with discrepancy well within 1σ . Bosonic operators C_{HD} and C_{HWB} are highly correlated in this case. Inclusion of Δ_{CKM} (matched to SMEFT at 1-loop level) shifts the best fit towards slightly higher values while simultaneously shrinking the allowed 2σ ranges. Discrepancies in A_l^{SLD} and A_b^{FB} continues to remain towards the higher side.

We then choose the set of operators motivated from Vectorlike lepton (VLL) model. Integrating out heavy degrees of freedom, at tree-level, generates the operators C_{He} , C_{Hl_1} and C_{Hl_3} . The allowed range for these WCs, after constraining using EWPO and Δ_{CKM} , turn out to be $\mathcal{O}(0.01)$. Inclusion of Δ_{CKM} (matched to SMEFT at 1-loop level) shifts allowed ranges to slightly larger values. We also explore a few minimal VLL frameworks and set the constraints over ratios of VLF Yukawas and the scale of the model. The posterior fit of the observables show that the pull for Γ_Z becomes worse with a discrepancy over 1.5σ . New posterior value of M_W is improved in comparison to SM, but the pull remains at $\sim 1.9\sigma$ and $\sim 2.4\sigma$ for the fits without and with Δ_{CKM} respectively. Thus we can conclude that minimal VLL frameworks are severely constrained by the precision measurements and slight tension exists with recent measurement of the M_W mass and A_b^{FB} .

Considering all the dimension-6 SMEFT operators, that appear in the EWPO at the leading order, only eight of the ten WCs, that appear at the tree-level, can be constrained by the EWPO. We compute their best fit, first with only EWPO and then including Δ_{CKM} (matched to SMEFT at 1-loop level). For the case of only EWPO, the best fit χ^2 becomes ~ 3 compared to a SM χ^2 value of 40. On the other hand, the inclusion of Δ_{CKM} makes the best fit $\chi^2 \sim 10.8$ compared to a SM χ^2 of 44. We also analyzed 2D correlations of the pairs of WCs with the highest correlation being between C_{Hl_3} and C_U . We find that SMEFT at the leading order brings the pulls for all the Electroweak observables within 1σ . Recent M_W measurement also fares exceptionally well with the pull coming down to $\sim -0.03\sigma$. However, the EWPO fit worsens the Δ_{CKM} compared to the SM as the discrepancy increases to -2.7σ . When the Δ_{CKM} constraint is also taken into the account in the fit, discrepancies in A_l^{SLD} , A_b^{FB} and A_c^{FB} go beyond 1σ while improving the agreement with Δ_{CKM} at -0.3σ . Overall, we can conclude that even after including the Δ_{CKM} into the fit, the pulls for all the observables are within 2σ with most them within 1σ .

Usage of the LEP-II data lifts the two blind directions which are otherwise present for the EWPO. These new observables correspond to the pair production of W 's, which subsequently leads to four fermion final states, resulting in a number of angular observables at various energies. For the case without including the Δ_{CKM} constraint, limits on the purely bosonic WCs C_{HD} and C_{HWB} are rather weak and their best-fit comes out to be slightly on the higher side. The correlations among the WCs are also generally on the higher side. The pulls, however, on the posterior values of the precision observables are very small showing excellent agreement with the experimental data. Like the previous 8 parameter fit, this also worsens the Δ_{CKM} by increasing the pull to -2.7σ . The inclusion of Δ_{CKM} constraint (matched to SMEFT at 1-loop level) in the fit constraints the WCs further, including that of C_{HD} and C_{HWB} along with simultaneously making their best-fit values smaller. Another peculiar aspect of this fit is that it makes the best-fit value of C_U very small. Correlations among the WCs still continues to be on the higher side and the agreement of the posterior values of the precision observables including Δ_{CKM} with the experimental data still remains excellent.

Our subsequent aim is to automatise this code with the current observables and make it available for public use very soon. Finally, in order to realise a true global fit, we would also be including the LHC observables in future.

Acknowledgments

The authors would like to thank Dr.Nilanjana Kumar for valuable discussions during the initial days of the work. M.T.A. acknowledges the financial support of Department of Science and Technology, Government of India, India (DST) through INSPIRE Faculty grant DST/INSPIRE/04/2019/002507. K.D. acknowledges Council for Scientific and Industrial Research (CSIR), India for JRF/SRF fellowship with the award letter no. 09/045(1654)/2019-EMR-I. K.D. also acknowledges the research Grant No. CRG/2018/004889 of the SERB, India, for the help with access to computers and accessories bought under the aegis of this grant. T.S. would like to acknowledge the support from the Dr. D.S. Kothari Postdoctoral fellowship scheme no. F.4-2/2006 (BSR)/PH/20-21/0163.

7 Appendix

The general correction to $\hat{\sigma}_h^0$ near the Z pole ($s - M_Z^2 \equiv \Delta$) in the SMEFT is

$$\frac{\delta\sigma_h^0}{\sigma_h^0} \simeq \frac{\delta\Gamma_{Z \rightarrow \ell\bar{\ell}}}{\Gamma_{Z \rightarrow \ell\bar{\ell}}} + \frac{\delta\Gamma_{Z \rightarrow Had}}{\Gamma_{Z \rightarrow Had}} - \frac{\delta\omega(M_Z^2)}{\omega(M_Z^2)} - \frac{\delta\omega^*(M_Z^2)}{\omega^*(M_Z^2)}. \quad (51)$$

where

$$\bar{w}(s) = s \frac{\bar{\Gamma}_Z}{\bar{M}_Z} \text{ we get : } \delta w(s) = s \left(\frac{(\Gamma_Z)_{SM}}{\hat{m}_Z} \right) \left(\frac{\delta\Gamma_Z}{(\Gamma_Z)_{SM}} \right). \quad (52)$$

$$\bar{w}(s) = \bar{\Gamma}_Z \bar{M}_Z \text{ we get : } \delta w(s) = (\Gamma_Z)_{SM} \hat{m}_Z \left(\frac{\delta\Gamma_Z}{(\Gamma_Z)_{SM}} \right). \quad (53)$$

but we note the following simplified expressions. In the SMEFT \bar{A}_f can be written as

$$\bar{A}_f = \frac{2\bar{r}_f}{1 + \bar{r}_f^2}, \quad (54)$$

where $\bar{r}_f = \frac{\bar{g}_V^f}{\bar{g}_A^f}$. The redefinition of the Z coupling then leads to a shift of \bar{A}_f such that $\bar{A}_f = (A_f)_{SM} \left(1 + \frac{\delta A_f}{(A_f)_{SM}} \right)$ where

$$\frac{\delta A_f}{(A_f)_{SM}} = \delta r_f \left(1 - \frac{2(r_f^2)_{SM}}{1 + (r_f^2)_{SM}} \right). \quad (55)$$

Here δr_f is defined by $r_f = (r_f)_{SM} (1 + \delta r_f)$ with $\delta r_f = \delta g_V^f / G_V^f - \delta g_A^f / G_A^f$. We again use : $(\dots)_{SM}$ for leading order SM predictions and $G_{A,V}^f$ for leading order SM predictions for the couplings.

References

- [1] **ATLAS** collaboration, G. Aad et al., *Observation of a new particle in the search for the Standard Model Higgs boson with the ATLAS detector at the LHC*, *Phys. Lett. B* **716** (2012) 1–29, [1207.7214].
- [2] T. Aoyama et al., *The anomalous magnetic moment of the muon in the Standard Model*, *Phys. Rept.* **887** (2020) 1–166, [2006.04822].
- [3] **Muon g-2** collaboration, B. Abi et al., *Measurement of the Positive Muon Anomalous Magnetic Moment to 0.46 ppm*, *Phys. Rev. Lett.* **126** (2021) 141801, [2104.03281].
- [4] D. Choudhury, K. Deka, S. Maharana and L. K. Saini, *Anomalous gauge couplings vis-à-vis $(g-2)_\mu$ and flavor observables*, *Phys. Rev. D* **106** (2022) 115026, [2203.04673].
- [5] K. Deka, S. Sadhukhan and M. P. Singh, *GeV Dark Matter in $U(1)_{L_\mu-L_\tau}$: Role of $(g-2)_\mu$ Anomaly*, 2203.17122.
- [6] J. Chakraborty, P. Ghosh, S. Mondal and T. Srivastava, *Reconciling $(g-2)$ and charged lepton flavor violating processes through a doubly charged scalar*, *Phys. Rev. D* **93** (2016) 115004, [1512.03581].
- [7] M. Du, J. Liang, Z. Liu and V. Q. Tran, *A vector leptoquark interpretation of the muon $g-2$ and B anomalies*, 2104.05685.
- [8] K. Ban, Y. Jho, Y. Kwon, S. C. Park, S. Park and P.-Y. Tseng, *A comprehensive study of vector leptoquark on the B -meson and Muon $g-2$ anomalies*, 2104.06656.
- [9] L. Darmé, M. Fedele, K. Kowalska and E. M. Sessolo, *Flavour anomalies and the muon $g-2$ from feebly interacting particles*, 2106.12582.
- [10] B. Bhattacharya, A. Datta, D. Marfatia, S. Nandi and J. Waite, *Axion-like particles resolve the $B \rightarrow \pi K$ and $g-2$ anomalies*, 2104.03947.
- [11] P. D. Group, R. L. Workman, V. D. Burkert, V. Crede, E. Klempt, U. Thoma et al., *Review of Particle Physics*, *Progress of Theoretical and Experimental Physics* **2022** (08, 2022) , [<https://academic.oup.com/ptep/article-pdf/2022/8/083C01/45434166/ptac097.pdf>]. 083C01.
- [12] **CDF** collaboration, T. A. et al. (CDF), *High-precision measurement of the W boson mass with the CDF II detector*, *Science* **376** (2022) 170.
- [13] L. Lehman and A. Martin, *Low-derivative operators of the Standard Model effective field theory via Hilbert series methods*, *JHEP* **02** (2016) 081, [1510.00372].
- [14] B. Henning, X. Lu, T. Melia and H. Murayama, *2, 84, 30, 993, 560, 15456, 11962, 261485, ...: Higher dimension operators in the SM EFT*, *JHEP* **08** (2017) 016, [1512.03433]. [Erratum: *JHEP* 09, 019 (2019)].
- [15] B. Grzadkowski, M. Iskrzynski, M. Misiak and J. Rosiek, *Dimension-Six Terms in the Standard Model Lagrangian*, *JHEP* **10** (2010) 085, [1008.4884].
- [16] D. C. Kennedy and B. W. Lynn, *Electroweak Radiative Corrections with an Effective Lagrangian: Four Fermion Processes*, *Nucl. Phys. B* **322** (1989) 1–54.

- [17] W. Buchmuller and D. Wyler, *Effective Lagrangian Analysis of New Interactions and Flavor Conservation*, *Nucl. Phys. B* **268** (1986) 621–653.
- [18] S. Weinberg, *Baryon and Lepton Nonconserving Processes*, *Phys. Rev. Lett.* **43** (1979) 1566–1570.
- [19] **ALEPH, DELPHI, L3, OPAL, SLD, LEP Electroweak Working Group, SLD Electroweak Group, SLD Heavy Flavour Group** collaboration, S. Schael et al., *Precision electroweak measurements on the Z resonance*, *Phys. Rept.* **427** (2006) 257–454, [hep-ex/0509008].
- [20] **ALEPH** collaboration, A. Heister et al., *Measurement of W-pair production in e^+e^- collisions at centre-of-mass energies from 183-GeV to 209-GeV*, *Eur. Phys. J. C* **38** (2004) 147–160.
- [21] **OPAL** collaboration, G. Abbiendi et al., *Measurement of the $e^+e^- \rightarrow W^+W^-$ cross section and W decay branching fractions at LEP*, *Eur. Phys. J. C* **52** (2007) 767–785, [0708.1311].
- [22] **L3** collaboration, P. Achard et al., *Measurement of the cross section of W-boson pair production at LEP*, *Phys. Lett. B* **600** (2004) 22–40, [hep-ex/0409016].
- [23] **ALEPH, DELPHI, L3, OPAL, LEP Electroweak** collaboration, S. Schael et al., *Electroweak Measurements in Electron-Positron Collisions at W-Boson-Pair Energies at LEP*, *Phys. Rept.* **532** (2013) 119–244, [1302.3415].
- [24] **ALEPH, CDF, D0, DELPHI, L3, OPAL, SLD, LEP Electroweak Working Group, Tevatron Electroweak Working Group, SLD Electroweak, Heavy Flavour Groups** collaboration, *Precision Electroweak Measurements and Constraints on the Standard Model*, 1012.2367.
- [25] A. Falkowski and F. Riva, *Model-independent precision constraints on dimension-6 operators*, *JHEP* **02** (2015) 039, [1411.0669].
- [26] B. Henning, X. Lu and H. Murayama, *How to use the Standard Model effective field theory*, *JHEP* **01** (2016) 023, [1412.1837].
- [27] L. Berthier and M. Trott, *Towards consistent Electroweak Precision Data constraints in the SMEFT*, *JHEP* **05** (2015) 024, [1502.02570].
- [28] L. Berthier and M. Trott, *Consistent constraints on the Standard Model Effective Field Theory*, *JHEP* **02** (2016) 069, [1508.05060].
- [29] I. Brivio and M. Trott, *The Standard Model as an Effective Field Theory*, *Phys. Rept.* **793** (2019) 1–98, [1706.08945].
- [30] J. Ellis, C. W. Murphy, V. Sanz and T. You, *Updated Global SMEFT Fit to Higgs, Diboson and Electroweak Data*, *JHEP* **06** (2018) 146, [1803.03252].
- [31] S. Dawson and P. P. Giardinò, *Electroweak and QCD corrections to Z and W pole observables in the standard model EFT*, *Phys. Rev. D* **101** (2020) 013001, [1909.02000].
- [32] S. Dawson, S. Homiller and S. D. Lane, *Putting standard model EFT fits to work*, *Phys. Rev. D* **102** (2020) 055012, [2007.01296].
- [33] J. Ellis, M. Madigan, K. Mimasu, V. Sanz and T. You, *Top, Higgs, Diboson and Electroweak Fit to the Standard Model Effective Field Theory*, *JHEP* **04** (2021) 279, [2012.02779].

- [34] **SMEFiT** collaboration, J. J. Ethier, G. Magni, F. Maltoni, L. Mantani, E. R. Nocera, J. Rojo et al., *Combined SMEFT interpretation of Higgs, diboson, and top quark data from the LHC*, *JHEP* **11** (2021) 089, [2105.00006].
- [35] I. Brivio and M. Trott, *Scheming in the SMEFT... and a reparameterization invariance!*, *JHEP* **07** (2017) 148, [1701.06424]. [Addendum: *JHEP* 05, 136 (2018)].
- [36] L. Berthier, M. Björn and M. Trott, *Incorporating doubly resonant W^\pm data in a global fit of SMEFT parameters to lift flat directions*, *JHEP* **09** (2016) 157, [1606.06693].
- [37] J. de Blas, Y. Du, C. Grojean, J. Gu, V. Miralles, M. E. Peskin et al., *Global SMEFT Fits at Future Colliders*, in *Snowmass 2021*, 6, 2022. 2206.08326.
- [38] J. de Blas, M. Pierini, L. Reina and L. Silvestrini, *Impact of the recent measurements of the top-quark and W-boson masses on electroweak precision fits*, 2204.04204.
- [39] C.-T. Lu, L. Wu, Y. Wu and B. Zhu, *Electroweak Precision Fit and New Physics in light of W Boson Mass*, 2204.03796.
- [40] A. Strumia, *Interpreting electroweak precision data including the W-mass CDF anomaly*, 2204.04191.
- [41] P. Asadi, C. Cesarotti, K. Fraser, S. Homiller and A. Parikh, *Oblique Lessons from the W Mass Measurement at CDF II*, 2204.05283.
- [42] A. Paul and M. Valli, *Violation of custodial symmetry from W-boson mass measurements*, 2204.05267.
- [43] J. Fan, L. Li, T. Liu and K.-F. Lyu, *W-Boson Mass, Electroweak Precision Tests and SMEFT*, 2204.04805.
- [44] E. Bagnaschi, J. Ellis, M. Madigan, K. Mimasu, V. Sanz and T. You, *SMEFT Analysis of m_W* , 2204.05260.
- [45] J. Gu, Z. Liu, T. Ma and J. Shu, *Speculations on the W-Mass Measurement at CDF*, 2204.05296.
- [46] M. Endo and S. Mishima, *New physics interpretation of W-boson mass anomaly*, 2204.05965.
- [47] R. Balkin, E. Madge, T. Menzo, G. Perez, Y. Soreq and J. Zupan, *On the implications of positive W mass shift*, 2204.05992.
- [48] R. S. Gupta, *Running away from the T-parameter solution to the W mass anomaly*, 2204.13690.
- [49] V. Cirigliano, W. Dekens, J. de Vries, E. Mereghetti and T. Tong, *Beta-decay implications for the W-boson mass anomaly*, 2204.08440.
- [50] S. Kanemura and K. Yagyu, *Implication of the W boson mass anomaly at CDF II in the Higgs triplet model with a mass difference*, 2204.07511.
- [51] J. Cao, L. Meng, L. Shang, S. Wang and B. Yang, *Interpreting the W mass anomaly in the vectorlike quark models*, 2204.09477.
- [52] P. Athron, A. Fowlie, C.-T. Lu, L. Wu, Y. Wu and B. Zhu, *The W boson Mass and Muon $g-2$: Hadronic Uncertainties or New Physics?*, 2204.03996.

- [53] J. M. Yang and Y. Zhang, *Low energy SUSY confronted with new measurements of W-boson mass and muon $g-2$* , 2204.04202.
- [54] G.-W. Yuan, L. Zu, L. Feng, Y.-F. Cai and Y.-Z. Fan, *Hint on new physics from the W-boson mass excess—axion-like particle, dark photon or Chameleon dark energy*, 2204.04183.
- [55] M. Blennow, P. Coloma, E. Fernández-Martínez and M. González-López, *Right-handed neutrinos and the CDF II anomaly*, 2204.04559.
- [56] S. Das Bakshi, J. Chakraborty and S. K. Patra, *CoDEx: Wilson coefficient calculator connecting SMEFT to UV theory*, *Eur. Phys. J. C* **79** (2019) 21, [1808.04403].
- [57] A. Dedes, J. Rosiek, M. Ryczkowski, K. Suxho and L. Trifyllis, *SmeftFR v3 – Feynman rules generator for the Standard Model Effective Field Theory*, 2302.01353.
- [58] I. Brivio, *SMEFTsim 3.0 — a practical guide*, *JHEP* **04** (2021) 073, [2012.11343].
- [59] J. Fuentes-Martin, P. Ruiz-Femenia, A. Vicente and J. Virto, *DsixTools 2.0: The Effective Field Theory Toolkit*, *Eur. Phys. J. C* **81** (2021) 167, [2010.16341].
- [60] A. Falkowski, B. Fuks, K. Mawatari, K. Mimasu, F. Riva and V. Sanz, *Rosetta: an operator basis translator for Standard Model effective field theory*, *Eur. Phys. J. C* **75** (2015) 583, [1508.05895].
- [61] S. Seviliano Muñoz, E. J. Copeland, P. Millington and M. Spannowsky, *FeynMG: a FeynRules extension for scalar-tensor theories of gravity*, 2211.14300.
- [62] A. Alloul, N. D. Christensen, C. Degrande, C. Duhr and B. Fuks, *FeynRules 2.0 - A complete toolbox for tree-level phenomenology*, *Comput. Phys. Commun.* **185** (2014) 2250–2300, [1310.1921].
- [63] V. Shtabovenko, R. Mertig and F. Orellana, *FeynCalc 9.3: New features and improvements*, *Comput. Phys. Commun.* **256** (2020) 107478, [2001.04407].
- [64] T. Hahn, *Generating Feynman diagrams and amplitudes with FeynArts 3*, *Comput. Phys. Commun.* **140** (2001) 418–431, [hep-ph/0012260].
- [65] W. Dekens and P. Stoffer, *Low-energy effective field theory below the electroweak scale: matching at one loop*, *JHEP* **10** (2019) 197, [1908.05295]. [Erratum: *JHEP* **11**, 148 (2022)].
- [66] J. Martinez-Martin and J. J. Sanz-Cillero, *Software tools for computing EW chiral amplitudes*, in *25th International Conference in Quantum Chromodynamics*, 11, 2022. 2211.12240.
- [67] M. E. Peskin and T. Takeuchi, *Estimation of oblique electroweak corrections*, *Phys. Rev. D* **46** (1992) 381–409.
- [68] I. Maksymyk, C. P. Burgess and D. London, *Beyond S, T and U*, *Phys. Rev. D* **50** (1994) 529–535, [hep-ph/9306267].
- [69] C. P. Burgess, S. Godfrey, H. Konig, D. London and I. Maksymyk, *Model independent global constraints on new physics*, *Phys. Rev. D* **49** (1994) 6115–6147, [hep-ph/9312291].
- [70] C. Csaki, J. Erlich and J. Terning, *The Effective Lagrangian in the Randall-Sundrum model and electroweak physics*, *Phys. Rev. D* **66** (2002) 064021, [hep-ph/0203034].

- [71] A. Dedes, W. Materkowska, M. Paraskevas, J. Rosiek and K. Suxho, *Feynman rules for the Standard Model Effective Field Theory in R -gauges*, *JHEP* **06** (2017) 143, [1704.03888].
- [72] A. Falkowski and K. Mimouni, *Model independent constraints on four-lepton operators*, *JHEP* **02** (2016) 086, [1511.07434].
- [73] A. Falkowski, M. González-Alonso and K. Mimouni, *Compilation of low-energy constraints on 4-fermion operators in the SMEFT*, *JHEP* **08** (2017) 123, [1706.03783].
- [74] Anisha, S. Das Bakshi, J. Chakraborty and S. K. Patra, *Connecting electroweak-scale observables to BSM physics through EFT and Bayesian statistics*, *Phys. Rev. D* **103** (2021) 076007, [2010.04088].
- [75] Z. Han and W. Skiba, *Effective theory analysis of precision electroweak data*, *Phys. Rev. D* **71** (2005) 075009, [hep-ph/0412166].
- [76] V. Cirigliano, J. Jenkins and M. Gonzalez-Alonso, *Semileptonic decays of light quarks beyond the Standard Model*, *Nucl. Phys. B* **830** (2010) 95–115, [0908.1754].
- [77] E. E. Jenkins, A. V. Manohar and P. Stoffer, *Low-Energy Effective Field Theory below the Electroweak Scale: Operators and Matching*, *JHEP* **03** (2018) 016, [1709.04486].
- [78] E. E. Jenkins, A. V. Manohar and P. Stoffer, *Low-Energy Effective Field Theory below the Electroweak Scale: Anomalous Dimensions*, *JHEP* **01** (2018) 084, [1711.05270].
- [79] **Particle Data Group** collaboration, R. L. Workman et al., *Review of Particle Physics*, *PTEP* **2022** (2022) 083C01.
- [80] A. Akhundov, A. Arbuzov, S. Riemann and T. Riemann, *The ZFITTER project*, *Phys. Part. Nucl.* **45** (2014) 529–549, [1302.1395].
- [81] M. Ciuchini, E. Franco, S. Mishima and L. Silvestrini, *Electroweak Precision Observables, New Physics and the Nature of a 126 GeV Higgs Boson*, *JHEP* **08** (2013) 106, [1306.4644].
- [82] M. Ciuchini, J. de Blas, E. Franco, D. Ghosh, S. Mishima, M. Pierini et al., *Updates on fits to electroweak parameters*, *PoS LeptonPhoton2015* (2016) 013.
- [83] J. de Blas, M. Ciuchini, E. Franco, S. Mishima, M. Pierini, L. Reina et al., *Electroweak precision observables and Higgs-boson signal strengths in the Standard Model and beyond: present and future*, *JHEP* **12** (2016) 135, [1608.01509].